



Distribution and sources of fallout ^{137}Cs and $^{239+240}\text{Pu}$ in equatorial and Southern Hemisphere reference soils

Gerald Dicen^{1,2}, Floriane Guillevic¹, Surya Gupta¹, Pierre-Alexis Chaboche^{3,4,5}, Katrin Meusburger⁶, Pierre Sabatier⁷, Olivier Evrard⁵, and Christine Alewell¹

¹Environmental Geosciences, Department of Environmental Science,
University of Basel, 4056 Basel, Switzerland

²Department of Science and Technology – Philippine Nuclear Research Institute (DOST-PNRI),
Commonwealth Avenue, Diliman, 1101 Quezon City, Philippines

³Japan Society for the Promotion of Science, Chiyoda-ku, Tokyo 102-0083, Japan

⁴Institute of Environmental Radioactivity, Fukushima University, Kanayagawa, Fukushima, Japan

⁵Laboratoire des Sciences du Climat et de l'Environnement (LSCE/IPSL),
Unité Mixte de Recherche 8212 (CEA-CNRS-UVSQ), Université Paris-Saclay, 91191 Gif-sur-Yvette, France

⁶Swiss Federal Institute for Forest, Snow and Landscape Research WSL,
8903 Birmensdorf, Zurich, Switzerland

⁷Laboratoire Environnements, Dynamiques et Territoires de Montagne (EDYTEM), CNRS,
Université Savoie Mont Blanc, 73376 Le Bourget-du-Lac, France

Correspondence: Gerald Dicen (gerald.dicen@unibas.ch)

Received: 31 October 2024 – Discussion started: 11 November 2024

Revised: 28 January 2025 – Accepted: 13 February 2025 – Published: 14 April 2025

Abstract. Past nuclear weapons testing (NWT) and nuclear power plant (NPP) accidents have resulted in the ubiquitous deposition of radionuclides in the environment. These fallout radionuclides (FRNs) are considered the privileged markers (“golden spikes”) of the Anthropocene stratigraphic layers. Their deposition in the 1950s coincided with the “Great Acceleration”, which is characterized by large-scale shifts in the Earth’s systems, including increased land-use change and soil degradation. Among the FRNs deposited globally, ^{137}Cs has been the most commonly used to assess soil erosion and/or the chronology of sediment deposition, while $^{239+240}\text{Pu}$ is an alternative soil erosion tracer and chronological marker that has been increasingly used due to a number of advantages.

We compiled ^{137}Cs and $^{239+240}\text{Pu}$ data published from undisturbed (so-called “reference”) soils in the equatorial and Southern Hemisphere regions to build a database within the framework of the AVATAR (A reVISED dATing framework for quantifying geomorphological processes during the Anthropocene) project. Using this database, named the AVATAR-Soils Database, we determined the distribution of ^{137}Cs and $^{239+240}\text{Pu}$ inventories in equatorial and Southern Hemisphere soils, along with the relative contributions of different fallout nuclear weapon sources by analyzing their isotopic ratios. Additionally, we demonstrated how the database can be used to identify the environmental factors that influence the distribution of ^{137}Cs and $^{239+240}\text{Pu}$ in reference soils by applying a machine learning algorithm.

Our meta-analysis revealed that high ^{137}Cs and $^{239+240}\text{Pu}$ inventories were recorded near the Equator and within the 20–40° S latitudinal bands, which coincide with the location of multiple NWT locations. The $^{240}\text{Pu}/^{239}\text{Pu}$ atomic ratios suggest that sources other than the global fallout (primarily from US and USSR weapon testing with a $^{240}\text{Pu}/^{239}\text{Pu}$ atomic ratio of ~ 0.18) contributed to the reference inventories in the Southern Hemisphere. These additional sources have been relatively neglected so far. Based on the $^{240}\text{Pu}/^{239}\text{Pu}$ atomic ratios, we have estimated that the French fallout contributed $\sim 20\%$ to the reference soil $^{239+240}\text{Pu}$ inventories in South America and up to 70 % in French Polynesia. In contrast, the British fallout contributed $\sim 27\%$ to the reference soil $^{239+240}\text{Pu}$ inventories in the rest of Oceania. Our machine learning algorithm identified the precipitation

of the coldest quarter, longitude, and latitude as the strongest predictors of the ^{137}Cs inventory. For the $^{239+240}\text{Pu}$ inventory, the mean diurnal temperature range, the annual temperature range, and the precipitation of the driest quarter were the strongest predictors. Altogether, these findings demonstrate the potential of the AVATAR-Soils Database as a resource for improving our understanding of the distribution and sources of ^{137}Cs and $^{239+240}\text{Pu}$ in equatorial and Southern Hemisphere soils and refining their application as tools in various Earth science research. The AVATAR-Soils Database may be accessed at <https://doi.org/10.5281/zenodo.14008221> (Dicen et al., 2024).

1 Introduction

1.1 Background

Radionuclide deposition from nuclear weapons testing (NWT) and nuclear power plant (NPP) accidents has become a global concern. Exposure to radionuclides can potentially lead to health problems and adverse ecological impacts because of the radiation hazards that they pose and the toxicity of many of these radionuclides (Owens et al., 2019; Bouville, 2020). Radionuclides are, therefore, considered to be serious environmental contaminants, especially those with long residence times. Despite the potential risks associated with them, fallout radionuclides (FRNs) with long half-lives provide the privileged markers (“golden spikes”) of the Anthropocene stratigraphic layers (Certini and Scalenghe, 2021). The onset of their deposition in the 1950s coincided with the “Great Acceleration”, which is characterized by large-scale shifts in the biophysical and socioeconomic components of the Earth system (Steffen et al., 2015), including an increase in soil degradation, mainly triggered by land-use change (Ferraro et al., 2018; Wang et al., 2022). The concentrations of FRNs and their isotopic ratios have been shown to provide reliable indicators of contamination sources (Alewell et al., 2014; Meusburger et al., 2020; Evrard et al., 2023), environmental impacts (Steinhauser et al., 2014; Foucher et al., 2023), sediment chronology (Bruel and Sabatier, 2020), sediment dating (de Lima Ferreira et al., 2016), soil redistribution (Alewell et al., 2017; Mabit et al., 2008), and particle transfers within soil profiles (Jagercikova et al., 2015) and, therefore, represent a major interest in Earth science research. Commonly studied FRNs include ^{241}Am ($t_{1/2} = 432.6$ years), ^{129}I ($t_{1/2} = 1.614 \times 10^7$ years), ^{14}C ($t_{1/2} = 5730$ years), ^3H ($t_{1/2} = 12.32$ years), ^{137}Cs ($t_{1/2} = 30.2$ years), ^{239}Pu ($t_{1/2} = 24\,110$ years), and ^{240}Pu ($t_{1/2} = 6563$ years). Among these, ^{137}Cs , ^{239}Pu , and ^{240}Pu have become particularly valuable as tracers in soil erosion studies because of their strong association with fine soil and sediment particles.

The ^{137}Cs artificial radionuclide, a fission product of plutonium and uranium, is one of the major byproducts of NWT and nuclear fuel burn-up, with a yield of more than 6 % (Kurihara et al., 2020). Owing to its relatively short half-life, ^{137}Cs is highly radioactive and is a source of both β - and γ particles. The plutonium isotope ^{239}Pu is either part of the fissile material in nuclear weapons and reprocessed nuclear

fuels or is formed when ^{238}U interacts with a neutron. The heavier plutonium isotope ^{240}Pu , considered an impurity in the fissile material of nuclear weapons (Şahin, 1981), is subsequently generated from ^{239}Pu through neutron capture as well. Both isotopes decay by α emission and have traditionally been measured by α spectrometry, which cannot effectively discriminate between their energies. Hence, ^{239}Pu and ^{240}Pu have been reported together as “ $^{239+240}\text{Pu}$ ”, and this nomenclature has likewise been applied throughout the paper.

While radioactive debris from NPP accidents was spread in the lower atmosphere, radioactive debris from NWT was introduced into the atmosphere at various heights depending on the type of nuclear testing conducted (e.g., barge/ship, balloon, airdrop, or air burst); the explosive yield of the bomb; and the weather conditions, including the amount and distribution of rainfall during redeposition. As opposed to NPP accidents, ^{137}Cs and $^{239+240}\text{Pu}$ from NWT are deposited more uniformly due to temperatures reaching far beyond the temperature of volatilization for Cs and Pu (Brode, 1964; Meusburger et al., 2020; Kirchner et al., 2011; Steinhauser et al., 2014) as well as the longer time frame in which differences in rainfall patterns are equalized. Upon explosion, radioactive substances rapidly attach to ambient aerosols and disperse according to airflow patterns (Bennett, 2002; Corcho-Alvarado et al., 2014). Aerosols with larger particle sizes ($> 50\,\mu\text{m}$) are deposited immediately within a few hundred kilometers of the blast, referred to as “local fallout”, and are considered to have limited global implications (Garcia Agudo, 1998; Bouisset et al., 2018). Debris injected into the troposphere remains suspended for up to a few weeks within the latitudinal band of injection, whereas debris injected into the stratosphere remains in circulation for up to a year (Bennett, 2002) or even longer for finer aerosol particles ($< 0.1\,\mu\text{m}$) (Corcho Alvarado et al., 2014). These radioactive particles find their way to the ground or surface water through wet and dry fallout deposition.

Among the host of FRNs deposited globally, ^{137}Cs has been the most commonly used tracer of soil erosion in the past (Walling, 1998; Walling et al., 2007; Mabit et al., 2013, 2014). However, more than 60 years after the fallout from NWT, which peaked in the 1960s, ^{137}Cs has undergone two half-lives and is now increasingly depleted and difficult to detect in many areas with relatively lower amounts of de-

position, such as the Southern Hemisphere. Its measurement now also increasingly requires the use of low-background analytical facilities. In addition, the heterogeneous inputs from NPP accidents in the Northern Hemisphere, such as those of Chernobyl, have resulted in highly variable ^{137}Cs inventories across Europe (Meusburger et al., 2020), especially across the Alps (Alewell et al., 2014). The latter is partly caused by the greater part of the Chernobyl deposition resulting from a few temporally and spatially very heterogeneous rainfall events. The ^{137}Cs deposition on the partly snow-covered ground also resulted in heterogeneous and concentrated flow patterns during snowmelt.

Owing to its longer half-life, $^{239+240}\text{Pu}$ has been increasingly recognized as an alternative tracer and chronological marker to assess soil erosion and/or the chronology of sediment deposition (Meusburger et al., 2023; Hancock et al., 2014; Alewell et al., 2017; Romanenko and Lujanienė, 2023). Globally, the spread of $^{239+240}\text{Pu}$ is also less affected by NPP accidents such as the Chernobyl and Fukushima incidents, which deposited $^{239+240}\text{Pu}$ mainly in confined proximal areas in Europe and up to ~ 200 km from the NPP site in Japan, respectively (Alewell et al., 2017). Although traces of $^{239+240}\text{Pu}$ (and other actinides) derived from Chernobyl were found in areas as far as Scandinavia and in the Baltic Sea, they remained minor compared with the contribution from NWT (Lin et al., 2021; Salminen-Paatero et al., 2020). As atmospheric NWT was also conducted throughout the year over several decades, this means that $^{239+240}\text{Pu}$ deposition due to NWT was more or less continuous, reducing the heterogeneity caused by deposition on snow-covered ground or the impact of a few heavy-rainfall events.

Upon deposition on land, evidence suggests that ^{137}Cs , similar to other monovalent ions, is rapidly and strongly adsorbed in the cation exchange sites of clay minerals to balance the negative charge on the aluminosilicate structure (Cornell, 1993; Mukai et al., 2016). The $^{239+240}\text{Pu}$ is (almost) irreversibly sorbed onto Fe/Mn oxides and/or forms complexes with organic matter (Kersting, 2013; Lujanienė et al., 2012), in addition to its adsorption onto clay particles. However, the exact sorption mechanisms and differences between ^{137}Cs and $^{239+240}\text{Pu}$ may be more complex and likely overlap depending on the deposition environment.

While the occurrence of ^{137}Cs and $^{239+240}\text{Pu}$ in the environment continues to be monitored globally, especially in areas with localized exposure to nuclear accidents, these FRNs have gained interest as powerful tools for investigating critical Earth surface processes because of their close association with the soil particles (Alewell et al., 2017; Mabit et al., 2013). Their deposition coinciding with the onset of the Great Acceleration also provides an opportunity to study the widespread land degradation that has been occurring since. However, our current scientific knowledge on the fallout chronology is better constrained in the Northern Hemisphere, whereas very little is known regarding the timing and the

spatial distribution of their deposition in the Southern Hemisphere (Foucher et al., 2021).

1.2 Objectives

The aim of this review and meta-analysis is to update our current knowledge on the distribution of fallout ^{137}Cs and $^{239+240}\text{Pu}$ in Southern Hemisphere soils as part of the Franco-Swiss-funded AVATAR project (<https://avatar-project.net/>, last access: 7 April 2025). The main objective of the AVATAR project is to better understand the fallout chronology and distribution of ^{137}Cs and $^{239+240}\text{Pu}$ in the Southern Hemisphere for various environmental applications. Here, we synthesized the history and origins of ^{137}Cs and $^{239+240}\text{Pu}$ in the Southern Hemisphere and identified gaps in the reported data. We then compiled reference soil ^{137}Cs and $^{239+240}\text{Pu}$ data from the literature to build a database. Using data from the literature, we determined the distribution of ^{137}Cs and $^{239+240}\text{Pu}$ and their possible sources using their isotopic ratios. Finally, we demonstrated in a case study how the database can be utilized to identify which environmental factors, such as climate, topography, and geographic location, affect the distribution of ^{137}Cs and $^{239+240}\text{Pu}$ in reference soils.

2 Origins of fallout ^{137}Cs and $^{239+240}\text{Pu}$ in Southern Hemisphere soils

In contrast to the Northern Hemisphere, where the Chernobyl or Fukushima NPP accidents influenced FRN deposition to a crucial extent in many regions, virtually all FRNs deposited in the Southern Hemisphere soils originate from the past atmospheric NWT carried out by different nuclear states (Fig. 1). The first NWT events occurred in 1945 with the Trinity Test atomic bomb testing in New Mexico by the USA, which yielded a total of 21 kt of energy and resulted in an 11 kt injection into the local/regional atmosphere and a 10 kt injection into the troposphere (UNSCEAR, 2000). As this relatively low-yield test was carried out atop a 30 m tower above 30°N , it can be assumed that none of the radioactive debris reached the Southern Hemisphere soils via wet and/or dry deposition. The 1945 bombings in Hiroshima and Nagasaki that followed after the Trinity Test, with yields of 21 and 15 kt, respectively, were detonated at a higher altitude (at 500–600 m). However, the yields were relatively minimal, causing the fallout to be more localized (Saito-Kokubu et al., 2007), and could not have significantly affected the Southern Hemisphere. Most NWT events that also occurred shortly after these were performed in the Northern Hemisphere until 1951 (Fig. 1).

Atomic and thermonuclear bombs differ fundamentally in their design. Atomic bombs exclusively utilize energy from the fission of fissile materials, which are primarily made up of ^{239}Pu or ^{235}U . The more powerful thermonuclear weapons obtain their yield from the fission of ^{239}Pu or ^{235}U in a

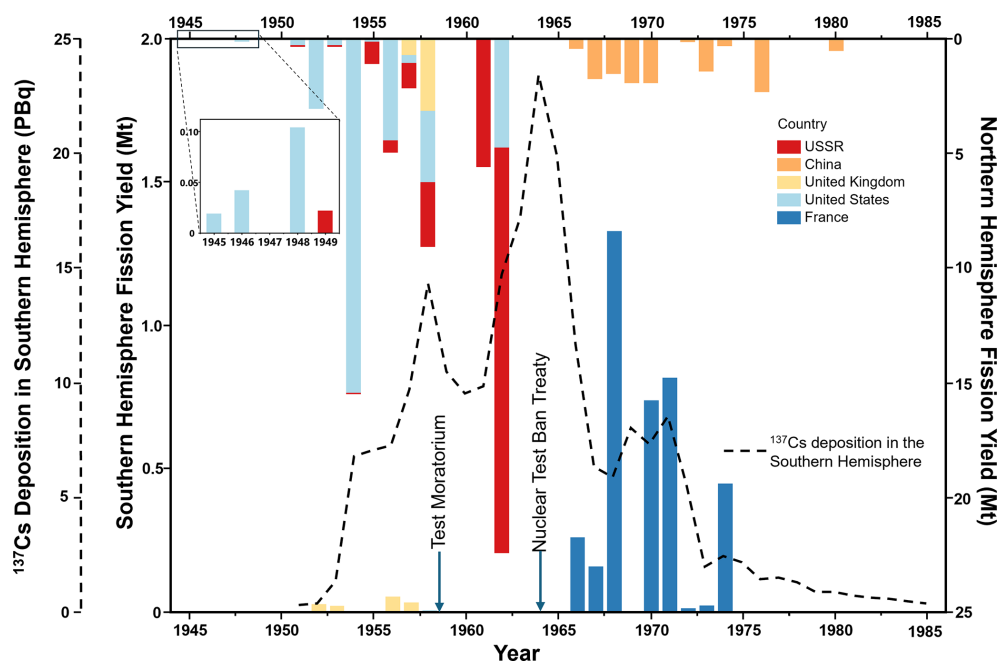


Figure 1. Fission yields of atmospheric nuclear weapons testing in the Northern Hemisphere and Southern Hemisphere (UNSCEAR, 2000) and ^{137}Cs deposition in the Southern Hemisphere (broken lines), which peaked at 23 PBq in 1964. Due to discontinuous monitoring by the United States Atomic Energy Commission's Environmental Measurements Laboratory between 1954 and 1976, 40 %–50 % of the data are missing (Evrard et al., 2020), casting a doubt on the fallout in the Southern Hemisphere. (Note that some very low-yield tests are not visible in the graph, including the French tests conducted in Algeria. For a complete list; see Annex C in UNSCEAR (2000). Axes for fission yields are also scaled differently for emphasis.)

primary stage, which then initiates fusion reactions of deuterium or tritium fuel in a secondary stage. Thermonuclear weapons contributed over 90 % of the radioactive debris from atmospheric NWT (UNSCEAR, 2000).

With the development of high-yield thermonuclear bombs in the 1950s, the majority of the radioactive debris from NWT was injected into the stratosphere and high equatorial atmosphere, equivalent to 139 and 6.36 Mt of fission energy, respectively (UNSCEAR, 2000). Upon settlement and mixing in the lower equatorial stratosphere, eddy diffusion allowed for the interhemispheric mixing of radioactive debris before deposition. The yield injected into the stratosphere and high equatorial atmosphere is much higher than the 15.6 Mt of equivalent fission energy injected into the troposphere, the debris of which remained more confined within a certain latitudinal band (UNSCEAR, 2000). The first high-yield thermonuclear weapon test, code-named “Ivy Mike”, was performed at Enewetak Atoll (11.55° N, 162.31° E) in November 1952, with a yield of 10.4 Mt (UNSCEAR, 2000). While this test was carried out in the Northern Hemisphere, its proximity to the Equator and its high yield resulted in FRN deposition in the Southern Hemisphere. Accordingly, radioactive fallout in the Southern Hemisphere likely only started after the Ivy Mike test in 1952, as was later observed in Antarctic ice cores by Koide et al. (1985).

Fission reactions produce most of the FRNs as byproducts, including ^{137}Cs . In addition, the yield from fission also provides an estimate of how much fissile material (^{239}Pu or ^{235}U) was used in the testing. On the other hand, fusion reactions mainly produce ^3H , ^{14}C , ^{54}Mn , and ^{55}Fe as FRNs (UNSCEAR, 2000), in addition to ^4He , neutrons, and large amounts of energy. Between 1945 and 1980, an estimated total of 502 atmospheric tests with a cumulative yield of 440 Mt were conducted globally, and more than 90 % of these tests were based in the Northern Hemisphere (UNSCEAR, 2000). Of the 440 Mt yield released, 189 Mt originated from fission (UNSCEAR, 2000), which is relevant for determining the amount of ^{137}Cs and $^{239+240}\text{Pu}$ released after a test. In the Northern Hemisphere, the majority of the fission yield was generated by NWT conducted by the USA and USSR. In contrast, those in the Southern Hemisphere, albeit much lower in terms of yield, were dominated by France (Fig. 1).

Gaps in reported data

According to the global monitoring network operated by the United States Atomic Energy Commission's Environmental Measurements Laboratory (EML), approximately 23.8 % of the fallout from all past atmospheric NWT was deposited in the Southern Hemisphere (UNSCEAR, 1982, 2000). This proportion was estimated from ^{90}Sr measurements in air fil-

ters, which served as a proxy for other FRNs such as ^{137}Cs and $^{239+240}\text{Pu}$ (see Annex C in UNSCEAR, 2000). However, as opposed to ^{137}Cs , the origin of fallout $^{239+240}\text{Pu}$ differs from that of ^{90}Sr . The ^{90}Sr and ^{137}Cs species are generated only in a series of fission chains, whereas $^{239+240}\text{Pu}$ is already part of the fissile material in nuclear weapons. Thus, using ^{90}Sr to estimate fallout $^{239+240}\text{Pu}$ can be expected to lead to inaccuracies in these calculations/reconstructions. This is especially true for the Southern Hemisphere, where fallout sources differ depending on location.

The deposition of FRNs in the Southern Hemisphere supposedly peaked in 1964–1965, based on the EML data, as reported by UNSCEAR (2000). However, 50 % of the data from EML monitoring stations were missing for 1954–1976 (Evrard et al., 2020), as most of the monitoring stations did not have continuous records for this period (Chaboche et al., 2021; Hardy, 1977). Thus, EML may not have accurately accounted for the fallout from French NWT, the emissions of which peaked in 1968. In addition, as most stations only began recording measurements between 1956 and 1958 (Hardy, 1977), the fallout from British NWT in Australia, which started in 1952 and 1953, may not have been considered. Therefore, the United Nations Scientific Committee on the Effects of Atomic Radiation (UNSCEAR) may have misestimated the fallout distribution in the Southern Hemisphere, especially in areas affected by the French and British fallout. A significant fraction of the Southern Hemisphere is also covered by oceans exposed to different precipitation regimes than terrestrial environments, and the fallout in these regions has not been monitored. These gaps in data for the Southern Hemisphere highlight the need to review and reevaluate the fallout in the Southern Hemisphere to refine the methods that rely on FRN data, especially those of ^{137}Cs and $^{239+240}\text{Pu}$.

3 Literature survey and analytical approaches

3.1 AVATAR-Soils Database: a database of ^{137}Cs and $^{239+240}\text{Pu}$ in equatorial and Southern Hemisphere reference soils

Using the Thomson Reuters Web of Science platform, we conducted a literature survey until October 2024 to build the AVATAR-Soils Database (<https://doi.org/10.5281/zenodo.14008221>, Dicen et al., 2024). The search keywords “soil”, “cesium”, “ ^{137}Cs ”, “Cs 137”, “plutonium”, “ $^{239+240}\text{Pu}$ ”, “Pu 239”, and “Pu 240” were used in isolation and/or combination with the names of the countries found in the Southern Hemisphere. All countries in South America and sub-Saharan Africa were included in the current literature survey to consider the NWT conducted near the Equator, to prevent discontinuity in continents whose areas cross the Equator, and to consider the seasonal movement of the Intertropical Convergence Zone (ITCZ) around the Equator. Publications in Portuguese and

Spanish languages and PhD dissertations that reported on soil ^{137}Cs and $^{239+240}\text{Pu}$ were also included in the selection.

For a soil profile to be included in the database, the following two conditions had to be satisfied: (i) the collection was from an undisturbed area, or the so-called “reference” site, located in a flat landscape that has, based on the best possible assessment, not been affected by soil redistribution processes such as erosion and/or deposition in recent decades or since the fallout period (Arata et al., 2017; Kirchner, 2013); (ii) the sampling details and site characteristics were provided.

Reported reference soils were excluded from the AVATAR-Soils Database if any of the following criteria were met: (a) soils were flooded, (b) soils were drained, (c) data were repeated from articles and/or applications already considered, (d) soils were located on a slope, (e) soils were located on a farm where cultivation had been implemented, and/or (f) the soil sampling locations were not provided or could not be obtained.

3.2 Statistical and modeling approaches

3.2.1 Decay correction for ^{137}Cs

To compare ^{137}Cs data spanning years or decades between measurements, all ^{137}Cs data were decay-corrected to 2024 using the following equation:

$$^{137}\text{Cs}_{2024} = ^{137}\text{Cs}_{\text{literature}} e^{-\lambda t}, \quad (1)$$

where λ is the decay constant of ^{137}Cs ($\lambda = \ln 2/30.2$ years) and t is the time in years since the sampling year. For ^{137}Cs data for which neither sampling dates nor decay correction dates were provided, we assumed a 4-year delay between the day of sampling and publication. This corresponds to the mean time delay between sampling and publication in the current literature survey and was calculated from articles in which both dates were provided. The same approach was applied by Chaboche et al. (2021) and Jagercikova et al. (2015) to decay-correct ^{137}Cs data for which the associated dates of sampling and decay correction were not available. To calculate the mean time delay in this study, we excluded data from a resampling study that spanned over decades (Loughran and Balog, 2006) from the calculation.

3.2.2 Latitudinal distribution comparisons

To compare the latitudinal distributions of the ^{137}Cs and $^{239+240}\text{Pu}$ inventories, inventory data were bootstrapped in R for 10 000 iterations (R Core Team, 2024). Bootstrapping is a resampling and replacement technique that allows inference from sample data without making strong distributional assumptions (Haukoos and Lewis, 2005; Mooney et al., 1993). It is, therefore, appropriate to compare datasets with large variations, such as the ^{137}Cs and $^{239+240}\text{Pu}$ inventories available from the AVATAR-Soils Database. The bootstrapped means, reported with the 95 % confidence interval, were compared with previously reported global data

analyzed from air filters (^{137}Cs derived from ^{90}Sr) and soil samples ($^{239+240}\text{Pu}$) by the EML (UNSCEAR, 2000; Hardy et al., 1973).

3.2.3 Two-source unmixing model

The isotopic ratios of FRN in the soil are affected by the isotopic signatures of the fallout sources (see Sect. 5.2). To unmix these sources, we used an unmixing model previously used to evaluate the contribution of fallout from two sources, where both global fallout and local/regional fallout have occurred at a given site (Kelley et al., 1999; Bouisset et al., 2021; Chaboche et al., 2021).

Isotopic ratios originating from low-yield tests, such as French and British NWT, result in low $^{240}\text{Pu}/^{239}\text{Pu}$ atomic ratios and $^{137}\text{Cs}/^{239+240}\text{Pu}$ activity ratios. As such, it is impossible to separate French fallout from British fallout based on these isotopic ratios. An assignment to either British or French NWT sources can be done depending on the location of the fallout origin, as it is known that, in the Southern Hemisphere, the French tests were performed in French Polynesia. In contrast, the British tests were conducted in Australia and the Malden Islands. However, the British testing in the Malden Islands was far enough from other equatorial and Southern Hemisphere land areas, with a wind direction towards the Equator (Chamizo et al., 2020), to not have had a significant fallout contribution in this part of the world.

When French or British fallout is mixed with the global fallout, the ratio R_s in the soil may, therefore, be expressed by the following equation:

$$R_s = x_{\text{B/FF}} \times R_{\text{B/FF}} + (1 - x_{\text{B/FF}}) \times R_{\text{GF}}, \quad (2)$$

where $R_{\text{B/FF}}$ is the ratio of either the British or French fallout, R_{GF} is the ratio of the global fallout, $x_{\text{B/FF}}$ is the relative contribution of the British or French fallout, and $(1 - x_{\text{B/FF}})$ is the relative contribution of the global fallout. The relative contribution of the British or French fallout may, therefore, be calculated via the following equation:

$$x_{\text{B/FF}} = \frac{R_s - R_{\text{GF}}}{R_{\text{B/FF}} - R_{\text{GF}}}. \quad (3)$$

The standard uncertainty in the contribution $u(x_{\text{B/FF}})$ was determined by the combination of uncertainties associated with each variable in Eq. (3) and is expressed as follows:

$$u(x_{\text{B/FF}}) = x_{\text{B/FF}} \times \sqrt{\left(\frac{u(R_s)}{R_s - R_{\text{GF}}}\right)^2 + \left(\frac{u(R_{\text{B/FF}})}{R_{\text{B/FF}} - R_{\text{GF}}}\right)^2 + \left(\frac{(R_s - R_{\text{B/FF}}) \times u(R_{\text{GF}})}{(R_s - R_{\text{GF}}) \times (R_{\text{B/FF}} - R_{\text{GF}})}\right)^2}. \quad (4)$$

3.2.4 Assessing inventory predictability in a case study with random forest

As FRNs have increasingly become an indispensable tool in many fields of scientific research, such as environmental

tracing and geomorphological studies, it is critical to obtain data in areas lacking data. One of the important aims of the AVATAR-Soils Database is the prediction of baseline ^{137}Cs and $^{239+240}\text{Pu}$ inventories in areas devoid of data. To achieve this goal, the predictability of the inventories in the current database has to be tested using possible explanatory variables or covariates.

Accordingly, geospatial and climatic variables, including rainfall, are considered the most important predictors of ^{137}Cs and $^{239+240}\text{Pu}$ deposition in the soil, as determined in previous studies (i.e., Chappell et al., 2011; Meusburger et al., 2020; Chaboche et al., 2021). We, therefore, used geospatial and historical bioclimatic variables (Table S1) as potential covariates in this case study. The historical bioclimatic data were extracted from WorldClim 2.1 climate data for 1970–2000 (Fick and Hijmans, 2017) at a 30 arcsec (~ 1 km) spatial resolution. A total of 22 potential covariates were used in this analysis, as detailed in Table S1. The correlations among and between these covariates and the inventories were tested via Spearman's rank correlation (Fig. S1).

A random forest algorithm (Breiman, 2001) was run in R (R Core Team, 2024) via the “ranger” package (Wright and Ziegler, 2017) to determine the best covariates that explain the variations in the ^{137}Cs and $^{239+240}\text{Pu}$ inventories while also showing the application of the AVATAR-Soils Database. The selection of the random forest model is based on existing studies that consistently use it as their first choice among various machine learning models (Hong et al., 2024; Shuryak, 2022; Gupta et al., 2022). The optimal value for the most sensitive hyperparameter, “mtry”, in the random forest model was determined using five-fold cross-validation. Default settings from the ranger package were used for the remaining hyperparameters, such as the number of trees, minimum node size, maximum tree depth, and splitting rule. In the cross-validation process, the data were randomly divided into five parts, each containing 20 % of the total data. The random forest model was trained five times. Each time, one of the parts was used as a validation set, while the others were used for training. The validation results were then combined and compared with the measured data to assess model accuracy. Model accuracy was evaluated via the root-mean-square error (RMSE), coefficient of determination (R^2), and concordance correlation coefficient (CCC) (Lawrence and Lin, 1989). This process was repeated for each mtry value to find the optimal value, and the entire cross-validation procedure was repeated three times to ensure robustness. The final correlation plot was created using the optimal mtry and averaged predictions from the three cross-validation repetitions. Additionally, the relative importance of each variable was evaluated via the residual sum of squares (RSS) metric (Gupta et al., 2021). A lower RSS indicates a more important covariate, with the second-lowest RSS identifying the second-most important covariate, and so on.

4 AVATAR-Soils Database overview

4.1 Publication distribution, trends, and applications

From the 1526 publications screened, only a total of 135 publications reporting 1122 reference soil profiles with ^{137}Cs and $^{239+240}\text{Pu}$ data were included in the database. Among these soil profiles, 999 (89.0 %) had ^{137}Cs data, 123 (11.0 %) had $^{239+240}\text{Pu}$ data, but only 29 (2.6 %) had both ^{137}Cs and $^{239+240}\text{Pu}$ data.

The earliest publication in the database on ^{137}Cs in equatorial and Southern Hemisphere reference soils is that of Loughran et al. (1988), who estimated soil erosion in a drainage basin in the Hunter Valley, New South Wales, Australia. Earlier publications on soil ^{137}Cs profiles, such as those of Loughran et al. (1982) and Campbell et al. (1982), were available, but the geographic locations of the investigated profiles were difficult to determine. Accordingly, they were excluded from the database. While publications on ^{137}Cs continued to increase in the following decades, the number of publications on $^{239+240}\text{Pu}$ increased only after the 2010s (Fig. 2a). For $^{239+240}\text{Pu}$, the earliest publication in the database was that conducted by Hardy et al. (1973), which was founded on the report released on the global inventory and the distribution of ^{238}Pu from SNAP-9A based on EML data (Hardy et al., 1972). While this was the first publication that aimed to reconstruct a regional-scale baseline fallout inventory of plutonium in the Southern Hemisphere, a subsequent study using the same set of samples was conducted by Kelley et al. (1999).

Most reference soil profiles across the equatorial and Southern Hemisphere land surfaces with ^{137}Cs data were located in South America (69.4 %). In comparison, Oceania (60.2 %) has the greatest number of $^{239+240}\text{Pu}$ measurements, mainly from Lal et al. (2020) and Hardy et al. (1973) (Fig. 2b). Despite sub-Saharan Africa covering a large portion of the equatorial and Southern Hemisphere land area, measurements of ^{137}Cs and $^{239+240}\text{Pu}$ in the region represent only 12.2 % and 17.1 % of all available data, respectively.

In terms of the applications for ^{137}Cs and $^{239+240}\text{Pu}$ measurements in reference soils, articles related to soil erosion assessment composed the majority of the publications, covering 68 % ($n=84$) of the total number; this was followed by applications related to environmental radioactivity (35 %, $n=43$) and applications for sediment tracing and fingerprinting (6 %, $n=7$). For ^{137}Cs publications, applications for soil erosion continued to increase until 2019 (Fig. 3), which implies the increased use of radionuclides for erosion assessment. While applications for environmental radioactivity assessment remain important for ^{137}Cs measurements in reference soils, they began to decrease after 2009. Environmental radioactivity publications in equatorial and Southern Hemisphere soils were driven primarily by the monitoring conducted by LaBrecque and coworkers (e.g., LaBrecque and Rosales, 1993, LaBrecque and Cordoves, 2007) of the

Venezuelan National Science and Technology Foundation (CONICET) following the Chernobyl NPP accident, and by Schuller et al. (1997a, b) across Chile after recording seemingly higher ^{137}Cs inventories than those previously estimated from the global weapons fallout. Despite ^{137}Cs being used by the sediment tracing and fingerprinting community (Evrard et al., 2020), ^{137}Cs measurements in reference soils for this application are uncommon. The ^{137}Cs data in source soils that have been eroded are more commonly reported alone, especially for large catchments where on-site erosion rates do not necessarily translate to the percent contribution of sediments in lakes, dams, and reservoirs because they can be stored in channels (Wallbrink et al., 1998). For example, only 10 % of the studies ($n=30$) in equatorial and Southern Hemisphere countries reviewed by Evrard et al. (2020) reported ^{137}Cs measurements in reference soils.

For the $^{239+240}\text{Pu}$ publications, studies in reference soils prior to 2000 were only conducted for environmental radioactivity assessment (Fig. 3). Everett et al. (2008) were the first to measure $^{239+240}\text{Pu}$ in equatorial and Southern Hemisphere reference soils for both soil erosion and sediment tracing applications, comparing its concentration with that of ^{137}Cs in the Herbert River catchment in Australia and its suitability as an alternative to ^{137}Cs . The suitability of using $^{239+240}\text{Pu}$ as a tracer for soils and sediments, as well as the development and improvement of measurement techniques, has driven the increase in the use of $^{239+240}\text{Pu}$ as a tracer for soil erosion (for an overview, see Alewell et al., 2017) and sediment transport (Romanenko and Lujanienė, 2023).

4.2 The ^{137}Cs and $^{239+240}\text{Pu}$ data availability in the literature

Among the 999 soil profiles analyzed for ^{137}Cs , 429 (42.9 %) had inventory data, 160 (16.0 %) had both inventory and activity data, 269 (26.9 %) had inventory data only, and 570 (57.0 %) had activity data only. Among the soil profiles with ^{137}Cs data, 297 (29.7 %) were decay-corrected to a particular date, 475 (47.5 %) had sampling dates provided, and 643 (64.3 %) had either the date of decay correction or the date of sampling. However, for 356 (35.6 %) of the published ^{137}Cs data, neither the date of decay correction nor the date of sampling was recorded.

For the 123 soil profiles analyzed for $^{239+240}\text{Pu}$, owing to the differences in the analytical techniques used, with techniques other than α spectrometry (i.e., inductively coupled plasma mass spectrometry – ICP-MS; thermal ionization mass spectrometry – TIMS; and accelerator mass spectrometry – AMS) being able to measure the two isotopes separately, some activity and inventory data had to be derived from the reported individual isotopes. In total, 102 (82.6 %) soil profiles had inventory data, 28 (22.8 %) had both inventory and activity data, 73 (71.6 %) had inventory data only, and 18 (14.6 %) had activity data only. The $^{240}\text{Pu}/^{239}\text{Pu}$ atomic ratio was either reported or derived for 91 (74.0 %)

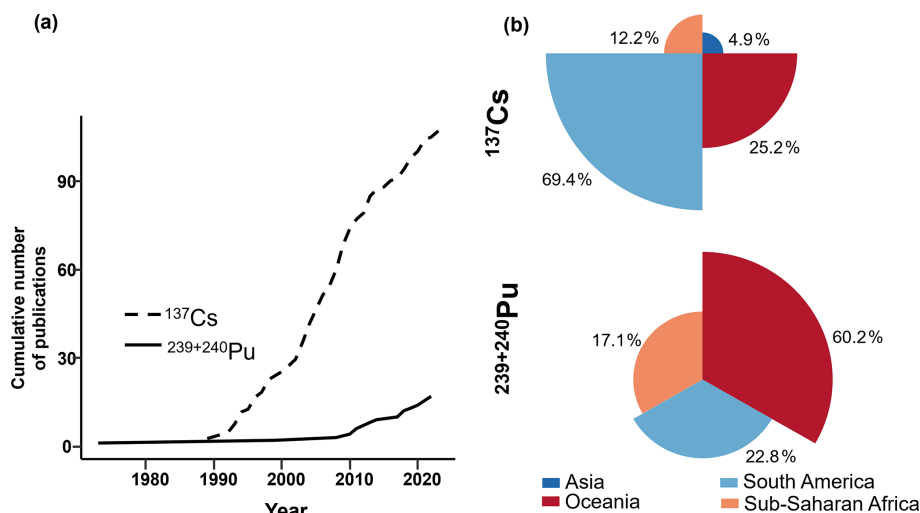


Figure 2. (a) The cumulative number of publications on ^{137}Cs ($n = 114$) and $^{239+240}\text{Pu}$ ($n = 21$) in equatorial and Southern Hemisphere reference soils and (b) the location of reference soil profiles with ^{137}Cs ($n = 999$) and $^{239+240}\text{Pu}$ ($n = 123$) measurements across equatorial and Southern Hemisphere continents.

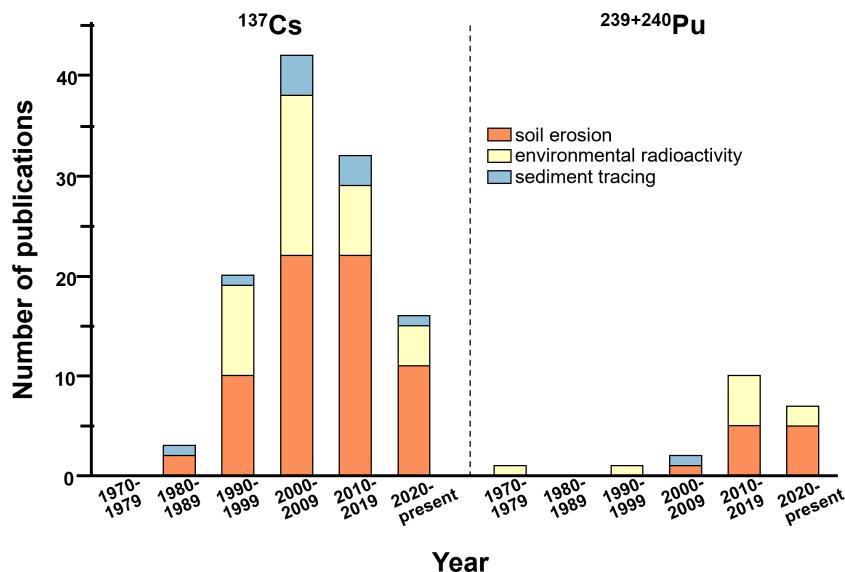


Figure 3. Temporal trends in publications using ^{137}Cs and $^{239+240}\text{Pu}$ data in reference soils for different applications.

soil profiles. The $^{137}\text{Cs}/^{239+240}\text{Pu}$ activity ratios were provided or derived for 24 (19.5 %) reference soil profiles.

5 Distribution and sources of the fallout ^{137}Cs and $^{239+240}\text{Pu}$ inventories

5.1 Distribution of the ^{137}Cs and $^{239+240}\text{Pu}$ inventories

The distributions of published ^{137}Cs and $^{239+240}\text{Pu}$ inventories in equatorial and Southern Hemisphere soils are located mostly along the edges of continents (Fig. 4). In contrast, little is known about inventories inside of continents, such as in northwestern Brazil or Bolivia in South America; in the

Democratic Republic of the Congo, Angola, Namibia, and Botswana in sub-Saharan Africa; and in the arid regions of central Australia.

As most of the NWT events occurred in the Northern Hemisphere, high ^{137}Cs inventories were recorded above the Equator (Fig. 5a, Table S2), mostly in sub-Saharan Africa. In the Southern Hemisphere latitudinal bands, relatively high ^{137}Cs inventories were recorded in South America, while lower ^{137}Cs inventories were recorded in Asia and Oceania, excluding Polynesia, which was at least partly directly and significantly affected by local fallout from the French NWT (Bouisset et al., 2021). For $^{239+240}\text{Pu}$ inventories (Fig. 5b,

Table S2), high values were also recorded in sub-Saharan Africa closest to the Equator, within the 0–10° N latitudinal band. For South America, high $^{239+240}\text{Pu}$ inventories were observed in the 30–40° S latitudinal band, and Polynesia had the highest inventories recorded, most likely because of its proximity to the French NWT grounds.

Based on the inventories compiled for the entire equatorial and Southern Hemisphere region in the AVATAR-Soils Database, the ^{137}Cs inventories were highest north of the Equator. In the Southern Hemisphere, ^{137}Cs inventories started to increase from the 20–30° S latitudinal band and peaked in the 40–60° S latitudinal bands (Fig. 6a). Furthermore, the $^{239+240}\text{Pu}$ inventories were the highest within the 0–10° and 20–30° S latitudinal bands, but they were the lowest above the Equator at 0–20° N (Fig. 6b). One of the reasons for these differences in the latitudinal distributions between the ^{137}Cs and $^{239+240}\text{Pu}$ inventories may be related to the differences in the locations of the sampled reference soils. For instance, in South America, the reference soils with ^{137}Cs inventory data are mainly located on the eastern side of the continent, while those with $^{239+240}\text{Pu}$ inventory data are mainly found more on the western side (Fig. 4). In sub-Saharan Africa, reference soils with ^{137}Cs inventories are mainly located in the northern part, whereas those with $^{239+240}\text{Pu}$ inventory data are mainly found more in the southern part. However, part of these differences in the distribution could also be a result of the different $^{137}\text{Cs}/^{239+240}\text{Pu}$ activity ratios of the fallout sources (see Sect. 5.2).

5.1.1 Comparison with previous fallout reconstructions

Fallout reconstructions based on actual reference soils have been conducted before to evaluate the global fallout distribution of ^{137}Cs inventories proposed by UNSCEAR (2000). At a global scale, previous work to reconstruct the fallout distribution from the literature was conducted by Aoyama et al. (2006). Regional-scale reconstructions of ^{137}Cs inventories in the Southern Hemisphere have previously been conducted by Chaboche et al. (2021) for South America and Chappell et al. (2011) for Australia. For $^{239+240}\text{Pu}$, Hardy et al. (1973) reported global $^{239+240}\text{Pu}$ baseline data from samples collected from 65 sites around the world by the EML, with 30 sites located in the Southern Hemisphere. Aliquots from 54 samples from these sites and two additional ones were reanalyzed by Kelley et al. (1999) to compare the baseline data generated with those obtained via novel analytical techniques.

The data compiled by Aoyama et al. (2006) suggest that, at the global scale, UNSCEAR (2000) underestimated the total fallout in the entire Northern Hemisphere down to 15° S but overestimated the total fallout within the 25–35° S latitudinal band (Aoyama et al., 2006), with no data available for further latitudinal bands. However, the dataset for the Southern Hemisphere in Aoyama et al. (2006) was based on only 7 publications and 66 soil profiles, which is extremely limited

with respect to providing reliable estimates for the entire land surface in this part of the world. Chaboche et al. (2021) also reported discrepancies between the fallout distribution proposed by UNSCEAR (2000) and the mean ^{137}Cs inventories in undisturbed soils in South America from the literature for each 10° latitude band. On the basis of compiled data from published research, ^{137}Cs inventories between 30 and 50° S were found to be higher than the proposed distribution by UNSCEAR (2000), while the ^{137}Cs inventories in soils were found to be lower between the 0 and 10° S latitudinal bands (Chaboche et al., 2021). Unlike Aoyama et al. (2006) and Chaboche et al. (2021), Chappell et al. (2011) reported that the latitudinal distribution proposed by UNSCEAR (2000) was in good agreement with the ^{137}Cs inventories measured in reference soil samples across Australia.

A comparison of the means per latitudinal band between the ^{137}Cs inventories compiled in the AVATAR-Soils Database and the distribution proposed by UNSCEAR (2000) is shown in Fig. 6a. The ^{137}Cs inventories generally agree in the equatorial region (10° N–10° S) and within the 50–50° S latitudinal bands. However, the distribution proposed by UNSCEAR (2000) is likely underestimated in the 10–20° N and 50–70° S latitudinal bands but overestimated in the 10–40° S latitudinal bands. Incidentally, the overestimated regions are also among the regions with the highest number of measurements reported in the literature. This implies that measurements done within these latitudinal bands during the period of discontinuous monitoring may have focused on areas with relatively higher fallout. On the other hand, the latitudinal bands with underestimated inventories from UNSCEAR (2000) have the lowest number of reference soil inventories. This indicates that more measurements may be needed to confirm whether the distribution proposed by UNSCEAR (2000) in these latitudinal bands is indeed inaccurate.

The means of the $^{239+240}\text{Pu}$ inventories compiled in the AVATAR-Soils Database appear to be higher over most of the Southern Hemisphere land surface (0–40° S; Fig. 6b) than those of the earlier estimates provided by the EML (Hardy et al., 1973). As these comparisons are based on a dataset that remains limited, more measurements of $^{239+240}\text{Pu}$ inventories are likely needed to better understand the distribution of fallout $^{239+240}\text{Pu}$ in equatorial and Southern Hemisphere reference soils.

5.2 Fallout sources

Although past atmospheric NWT events were mostly conducted in the Northern Hemisphere, a considerable part of their debris was also deposited in the Southern Hemisphere because of their long residence time, long-range transport, and atmospheric mixing. Thus, one of the primary sources of fallout ^{137}Cs and $^{239+240}\text{Pu}$ in Southern Hemisphere soils includes the NWT dominated by the USA and USSR (referred to as the “global fallout”; Table 1). This occurred in addi-

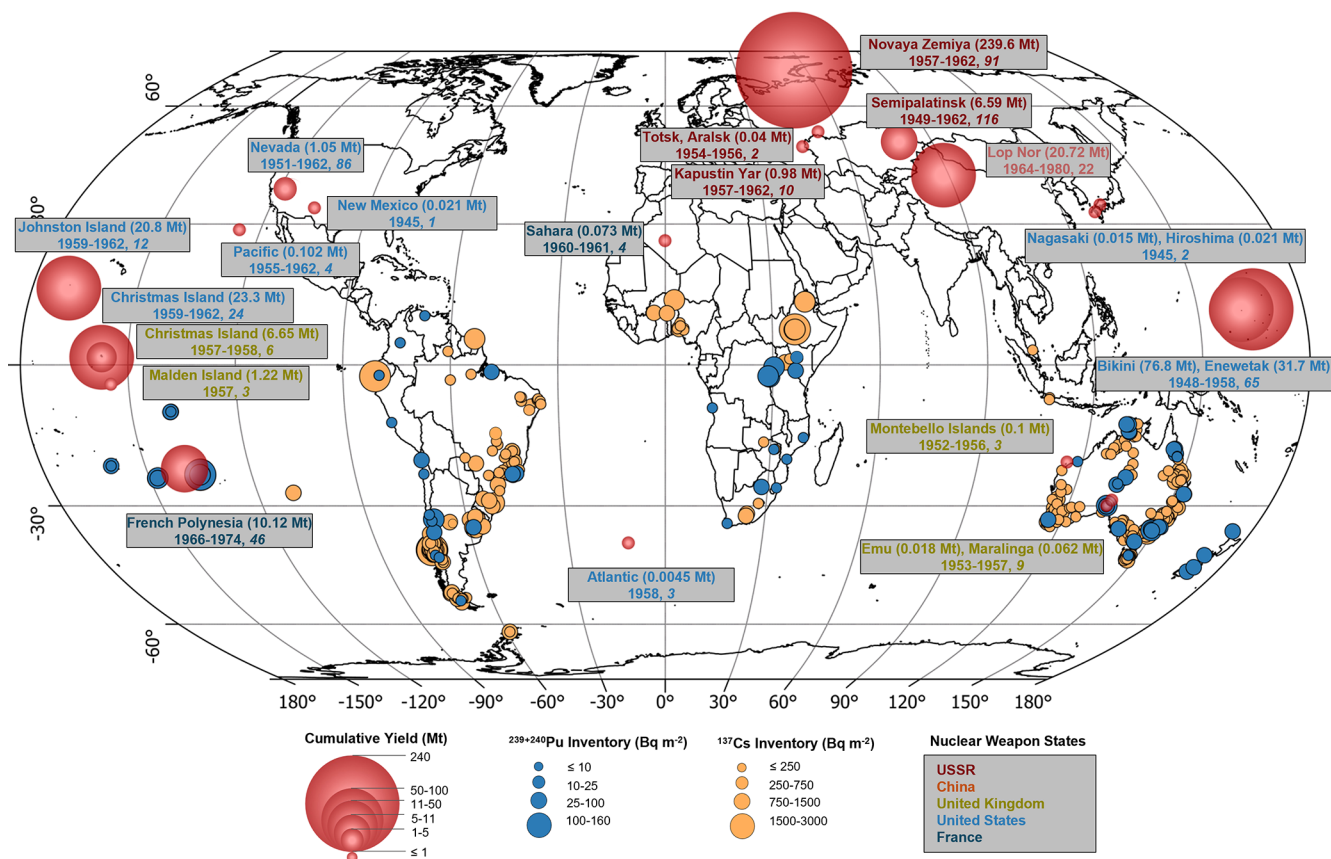


Figure 4. Cumulative yield of global atmospheric nuclear weapon detonations (modified from Chaboche et al., 2021) and FRN (^{137}Cs and $^{239+240}\text{Pu}$) inventories in equatorial and Southern Hemisphere reference soils. Does not include the Vixen B series in Australia, which used 22 kg plutonium (Johansen et al., 2014). The ^{137}Cs inventories were decay-corrected to 2024.

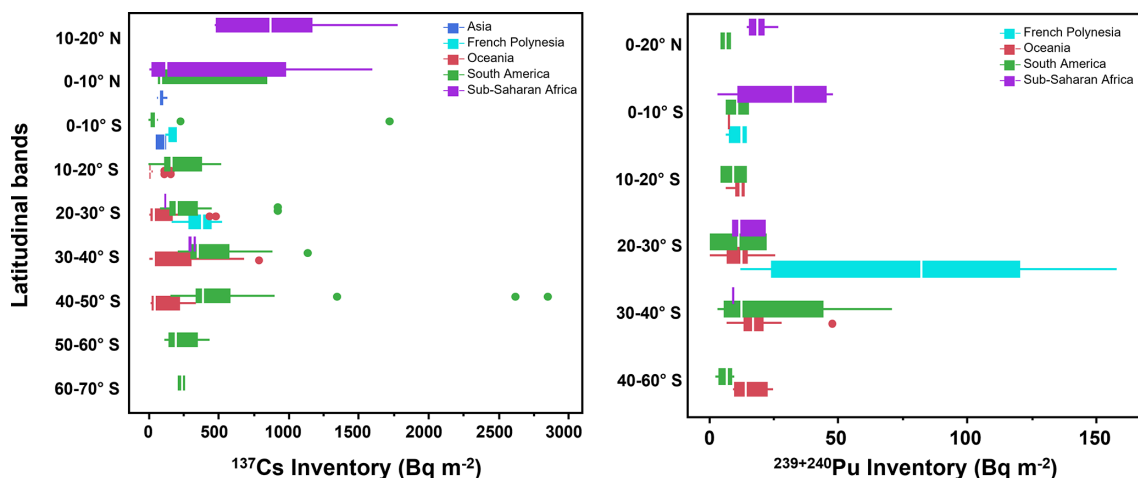


Figure 5. Box plots of the latitudinal distribution of ^{137}Cs and $^{239+240}\text{Pu}$ inventories in reference soils, classified per continent. Inventories from French Polynesia are grouped together. The mean, median, 25th percentile, and 75th percentile values are presented in Table S2.

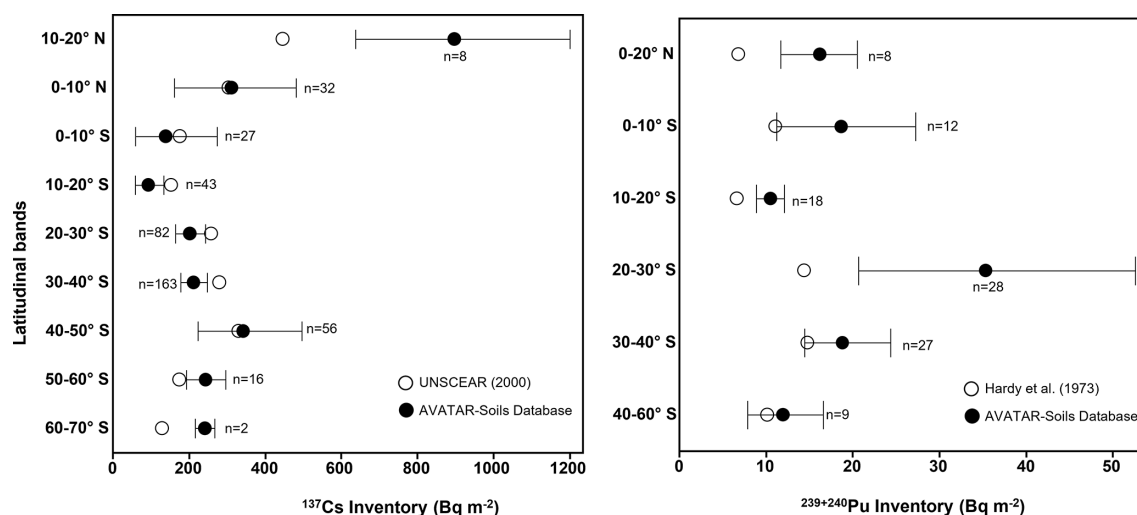


Figure 6. Latitudinal band comparisons of ^{137}Cs and $^{239+240}\text{Pu}$ inventories between the AVATAR-Soils Database and EML, as reported by UNSCEAR (2000) for ^{137}Cs and Hardy et al. (1973) for $^{239+240}\text{Pu}$. Error bars are the 95 % confidence intervals of the means simulated using 10 000 bootstrapped iterations in R. The numbers indicated correspond to the number of reference soil inventories in the AVATAR-Soils Database.

tion to fallout derived from the generally low-yield NWT conducted in the Southern Hemisphere, such as the French NWT in French Polynesia (referred to as the “French fallout”) and NWT performed by the UK in Australia (referred to as the “British fallout”). A distinct signature of the earlier NWT dominated by the USA before the test moratorium was signed in 1958 was also documented in dated ice cores in the Southern Hemisphere (Koide et al., 1979, 1985) and is referred to as the “pre-moratorium fallout”.

5.2.1 Isotopic fingerprints of fallout sources

Weapons-grade plutonium generally contains more than 93 % of ^{239}Pu , which is equivalent to a $^{240}\text{Pu}/^{239}\text{Pu}$ atomic ratio below 0.07 (Warneke et al., 2002; Ketterer and Szechenyi, 2008; Jones, 2019). However, this atomic ratio changes in the resulting fallout due to nuclear transformations upon fission and the capture of fast neutrons by ^{238}U in fusion devices (Hancock et al., 2014). Thus, due to the different weapon types and designs used by the different nuclear weapon states, each fallout source has its own distinct isotopic signature (Table 1). Low-yield detonations result in fallout with low $^{240}\text{Pu}/^{239}\text{Pu}$ atom ratios, whereas high-yield detonations (characteristic of thermonuclear bombs) result in high $^{240}\text{Pu}/^{239}\text{Pu}$ atomic ratios due to high neutron fluxes (Corcho-Alavarado et al., 2022; Buesseler, 1997; Lachner et al., 2010). Notably, these isotope fractionations do not differ depending on whether the FRNs are injected into the troposphere or the stratosphere (Bouisset et al., 2021).

Global fallout has a $^{240}\text{Pu}/^{239}\text{Pu}$ atomic ratio of ~ 0.18 , as determined from soil samples collected from 1970 to 1971 from regions around the world that were not influenced by plumes from low-yield NWT events, which is not character-

istic of samples collected during this period (Kelley et al., 1999). Other researchers have reported similar values elsewhere in the Northern Hemisphere (Meusburger et al., 2016, 2018, 2020; Krey et al., 1976; McArthur and Miller, 1989; Krey and Beck, 1981). As the global fallout $^{240}\text{Pu}/^{239}\text{Pu}$ signature was measured in soils collected from 1970 to 1971, it can be assumed that these soils also contained the plutonium from the pre-moratorium fallout. However, the $^{240}\text{Pu}/^{239}\text{Pu}$ atom ratio of ~ 0.18 is also in agreement with the measurements conducted on air filters collected for the 1959–1970 period (HASL, 1973, as cited in Bertine et al., 1986; Koide et al., 1985). These findings suggest that the pre-moratorium fallout did not significantly contribute to soil $^{239+240}\text{Pu}$ inventories. Recent investigations of freshwater lakes in the Southern Hemisphere also suggest that the pre-moratorium fallout contribution is much lower than that of other fallout sources (Guillevic et al., 2025).

The French fallout signature is characterized by a much lower $^{240}\text{Pu}/^{239}\text{Pu}$ atomic ratio of ~ 0.035 , based on different measurements of samples collected from French Polynesia (IAEA 1998; Hrnccek et al., 2005; Chiappini et al., 1996). It is important to note, however, that this signature is only representative of tests and safety trials, which resulted in local fallout at the Mururoa and Fangataufa NWT sites (Table S3). This signature is used as a reference because it is the only one published to date, and no known signatures are available for the 37 other balloon-based nuclear tests, including the thermonuclear ones. For the British fallout, similarly low $^{240}\text{Pu}/^{239}\text{Pu}$ atomic ratios of ~ 0.04 have also been determined on samples collected near the Australian testing sites (Child and Hotchkis, 2013; Johansen et al., 2014, 2019; Tims et al., 2013b). These low $^{240}\text{Pu}/^{239}\text{Pu}$ atomic ratios are

Table 1. Summary of ²³⁹Pu/²⁴⁰Pu atomic ratios and ¹³⁷Cs/²³⁹⁺²⁴⁰Pu activity ratios reported from the literature. A compilation of the values reported for each publication are presented in Table S3.

Fallout source	Nuclear states responsible	Period of testing	Measurement location	²⁴⁰ / ²³⁹ Pu atomic ratio	References	¹³⁷ Cs/ ²³⁹⁺²⁴⁰ Pu activity ratio	References
Pre-moratorium fallout	USA (more dominant) and USSR	1945–1958	Arctic	0.24 ± 0.03	Koide et al. (1985)	11.88	Koide et al. (1982)
			Antarctic	0.29 ± 0.05	Koide et al. (1985)	10.76 ± 1.08	Koide et al. (1979, 1982)
British fallout	UK	1952–1958	Australia	0.042 ± 0.015	Child and Hotchkis (2013), Johansen et al. (2014, 2019), and Tims et al. (2013b)	0.269 ± 0.088	Tims et al. (2013b) and Johansen et al. (2019)
Global fallout	USSR (more dominant) and USA	1958–1963	Northern Hemisphere	0.18 ± 0.004	Kelley et al. (1999), Meusburger et al. (2016, 2018, 2020), Krey et al. (1976), McArthur and Miller (1989), and Krey and Beck (1981)	20.20 ± 1.96	McArthur and Miller (1989); Meusburger et al. (2016); Krey and Beck (1981); Hodge et al. (1996); Hardy (1975); Kim et al. (1998); de Bortoli et al. (1968); HASL, 1973, as cited in Bertine et al. (1986); and Earkins et al., 1981, as cited in Hodge et al. (1996)
			Southern Hemisphere	0.18 ± 0.008	Kelley et al. (1999)		
French fallout	France	1964–1974	French Polynesia	0.035 ± 0.015	Hrnecek et al. (2005), Chiappini et al. (1999), Chiappini et al. (1996), Chiappini et al. (1998), and Bouisset et al. (2021)	1.74 ± 0.035	Bouisset et al. (2021)

indeed characteristic of the low-yield NWT events that occurred 15 years apart. Importantly, among the fallout source isotopic signatures, only the global fallout was supported by measurements of air filter samples (Table S3). Therefore, the ratios determined from the soil or sediment samples may have received minor contributions from sources other than the local source to which these ratios were attributed. Nevertheless, these isotopic ratios still provide useful tools for estimating the sources of fallout ²³⁹⁺²⁴⁰Pu in different environmental compartments globally.

Another indicator of the origin of FRN fallout is the ¹³⁷Cs/²³⁹⁺²⁴⁰Pu activity ratio, assuming that ¹³⁷Cs and ²³⁹⁺²⁴⁰Pu are sorbed tightly to soil particles even after several decades. Reference soils in Colorado, which were reported to have mainly received radionuclides from the global fallout (as opposed to other sources of contamination, such as plutonium processing plant fallout), had a ¹³⁷Cs/²³⁹⁺²⁴⁰Pu activity ratio of ~ 20 (decay-corrected to 2024 for the current study; Hodge et al., 1996; Price 1991). Similar ratios have been reported elsewhere in the USA (McArthur and Miller, 1989; Krey and Beck, 1981; Hodge et al., 1996; Hardy 1975), in Italy (de Bortoli et al., 1968), in Scotland (Earkins et al., 1981, as cited in Hodge et al., 1996), and in South Korea (Kim et al., 1998). However, Meusburger et al. (2016) reported a considerably higher variation in the ¹³⁷Cs/²³⁹⁺²⁴⁰Pu activity ratio in the Hae-an catchment, adjacent to the demilitarized zone in South Korea (Table S3). This is due to the different adsorption behaviors of ²³⁹⁺²⁴⁰Pu and ¹³⁷Cs in the soil, with ²³⁹⁺²⁴⁰Pu migrating to deeper layers than ¹³⁷Cs (Meusburger et al., 2016). For the French fall-

out, only Bouisset et al. (2021) provided a ¹³⁷Cs/²³⁹⁺²⁴⁰Pu activity ratio of ~ 1.7, which was calculated in the same way as their proposed ²⁴⁰Pu/²³⁹Pu atomic ratio. Similarly, Tims et al. (2013b) and Johansen et al. (2019) also reported low ¹³⁷Cs/²³⁹⁺²⁴⁰Pu activity ratios of 0.17 and 0.32 near the Australian testing sites in Maralinga and the Montebello Islands, respectively. However, due to the limited measurements of ¹³⁷Cs/²³⁹⁺²⁴⁰Pu activity ratios other than those characterizing the global fallout, as well as the differences in migration patterns between ²³⁹⁺²⁴⁰Pu and ¹³⁷Cs in the soil, these ratios must be used with caution. To determine the ¹³⁷Cs/²³⁹⁺²⁴⁰Pu activity ratios of the different sources more accurately, we propose that more reliable matrices that preserve the original ratio must be used, taking radioactive decay into account. These matrices could include coral archives or undisturbed rain gauge lake sediments where the percentage of the global fallout is known.

Owing to the high uncertainty associated with the ¹³⁷Cs/²³⁹⁺²⁴⁰Pu activity ratios, only the ²⁴⁰Pu/²³⁹Pu atomic ratios were used to determine the fallout sources in the AVATAR-Soils Database. In addition, data on the ¹³⁷Cs/²³⁹⁺²⁴⁰Pu activity ratios were only available for 14 reference soils, which were collected near the testing sites in French Polynesia and in Maralinga. This approach is extremely insufficient for determining the sources of ¹³⁷Cs and ²³⁹⁺²⁴⁰Pu in the large parts of the equatorial and Southern Hemisphere regions.

5.2.2 The $^{240}\text{Pu}/^{239}\text{Pu}$ atom ratios of reference soils

As shown in Fig. 7, the $^{240}\text{Pu}/^{239}\text{Pu}$ atomic ratios of the French and British fallout overlap with each other. Although it has been shown that the French fallout is responsible for the shift in the $^{240}\text{Pu}/^{239}\text{Pu}$ atom ratios from the global fallout in South America (Chaboche et al., 2021), it is not known whether it significantly contributed to the shifts in the $^{240}\text{Pu}/^{239}\text{Pu}$ atomic ratios in other regions. It was, therefore, assumed that contributions from the French fallout caused deviations in the $^{240}\text{Pu}/^{239}\text{Pu}$ atomic ratios from the global fallout in South America and French Polynesia (e.g., Chaboche et al., 2021; Bouisset et al., 2021), while the British fallout caused similar deviations in the rest of Oceania (Froehlich et al., 2019; Tims et al., 2013a).

The $^{240}\text{Pu}/^{239}\text{Pu}$ atomic ratios near the Equator and below 45°S in the AVATAR-Soils Database (Fig. 7) are more characteristic of the global fallout signature. However, along the midlatitudes ($20\text{--}45^\circ\text{S}$), a mixture can be observed, with many of the points displaying shifts in the $^{240}\text{Pu}/^{239}\text{Pu}$ atomic ratios towards either the French or British fallout. Among the continents, only reference soils from sub-Saharan Africa showed $^{240}\text{Pu}/^{239}\text{Pu}$ atomic ratios that were exclusively attributable to the global fallout. The majority of those collected from South America and Oceania deviated from the global fallout signature, with an expected significant contribution of low-yield NWT fallout in French Polynesia and Australia.

The reference soil profiles with the lowest $^{240}\text{Pu}/^{239}\text{Pu}$ atom ratios (0.0394 ± 0.0062), characteristic of low-yield fallout, were those collected from the Gambier archipelago (23°S , 135°W), which is located 425 km from the French testing sites of Moruroa (22.2°S , 138.7°W) and Fangataufa (21.8°S , 138.9°W) in French Polynesia (Bouisset et al., 2021). Interestingly, comparable $^{240}\text{Pu}/^{239}\text{Pu}$ atomic ratios were also reported in reference soils collected from western Chile and Australia. Chamizo et al. (2011) reported a ratio of 0.041 ± 0.003 at a high-altitude site in La Parva, Chile (33°S , 70°W), whereas Lal et al. (2017) reported a $^{240}\text{Pu}/^{239}\text{Pu}$ atomic ratio of 0.069 ± 0.005 in central Australia (25.3°S , 132.0°E), which is close to the values measured in soils near the UK testing sites in the Montebello Islands (0.045 ± 0.002) and Maralinga ($0.04\text{--}0.05$) (Tims et al., 2013a, b). Therefore, all of these regions showed the highest contribution from either French or British fallout. For the rest of the equatorial and Southern Hemisphere region, the global fallout was considered to be the main source of $^{239+240}\text{Pu}$ (Fig. 8).

5.2.3 Relative contributions of fallout sources to FRN inventories

The relative contributions of the fallout sources calculated from the $^{240}\text{Pu}/^{239}\text{Pu}$ atomic ratios in South America and Oceania are shown in Fig. 8. Again, we assumed that only the

contributions from the French NWT caused deviations in the ratios from the global fallout in South America and French Polynesia, whereas the British NWT caused deviations in the rest of Oceania. The French fallout had a significant contribution between 20 and 40°S in South America, which is approximately the same latitudinal band in which the French NWT events were conducted in Polynesia. In Australia, a significant contribution of the British fallout was observed in the central and western parts of the country, in areas located near and between the testing sites in Emu, Maralinga, and the Montebello Islands at $15\text{--}35^\circ\text{S}$. On average, the French fallout contributed $\sim 20\%$ to the reference soil $^{239+240}\text{Pu}$ inventories in South America and $\sim 68\%$ in French Polynesia, whereas the British fallout contributed $\sim 27\%$ to the reference soil $^{239+240}\text{Pu}$ inventories in the rest of Oceania. The uncertainties associated with the relative contributions in each soil profile, as well as the relative contributions in areas not shown on the map, calculated using Eq. (4), can be found in Table S4. These uncertainties were calculated by propagating the uncertainties associated with the fallout source $^{240}\text{Pu}/^{239}\text{Pu}$ atomic ratios and the ratios in the soil. However, the nature of the distribution of $^{239+240}\text{Pu}$ in the Southern Hemisphere could provide another source of uncertainty.

As opposed to the Northern Hemisphere, the influence of the French and British fallout in the Southern Hemisphere led to some heterogeneity in $^{240}\text{Pu}/^{239}\text{Pu}$ atomic ratios in the soil (Kelley et al., 1999; Chamizo et al., 2011; Chamizo et al., 2020). This is due to the low fallout spread over multidecadal weapon development and the significant tropospheric debris content, which is less homogeneous than stratospheric fallout, integrated in the soil (Kelley et al., 1999). For example, a wide variability in $^{240}\text{Pu}/^{239}\text{Pu}$ atomic ratios was observed by Chamizo et al. (2011) in Chile within the $20\text{--}40^\circ\text{S}$ range, which encompasses the latitude of the French NWT in French Polynesia. In Madagascar, a similar, although less pronounced, variability was also observed in peat and marshland cores (Chamizo et al., 2020). Interestingly, the cores with the lowest ^{239}Pu inventories had $^{240}\text{Pu}/^{239}\text{Pu}$ atomic ratios significantly lower than the global fallout signature. However, as the studied sites are marshlands subjected to flooding regimes (Chamizo et al., 2020), factors other than atmospheric fallout likely affected the distribution of Pu in the area. For the same reason, the ^{210}Pb chronology could not be established in the peat layers.

Upon comparing the $^{240}\text{Pu}/^{239}\text{Pu}$ atomic ratios analyzed from 5 g aliquots of soils with thermal ionization mass spectrometry (TIMS), Kelley et al. (1999) also observed a $\pm 16\%$ standard deviation from the ratios previously obtained from 1 kg aliquots of the same samples by Krey et al. (1976). This is higher than the $\pm 6\%$ standard deviation observed in samples collected from the Northern Hemisphere (Kelley et al., 1999). This indicates that sample heterogeneity could also affect $^{240}\text{Pu}/^{239}\text{Pu}$ atomic ratios and may not fully reflect the actual contribution from different fallout sources.

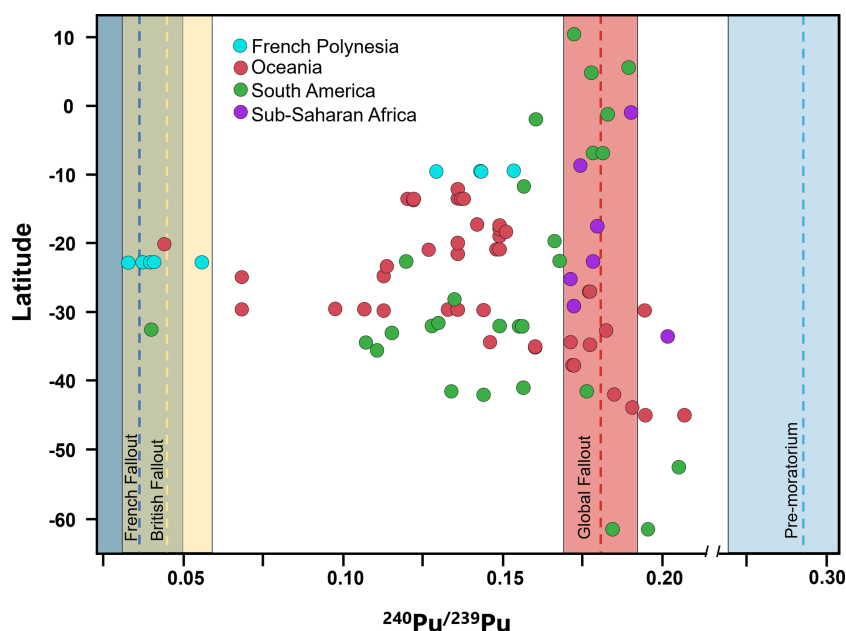


Figure 7. Latitudinal distribution of the $^{240}\text{Pu}/^{239}\text{Pu}$ atomic ratios in reference soils in comparison to the known fallout source ratios.

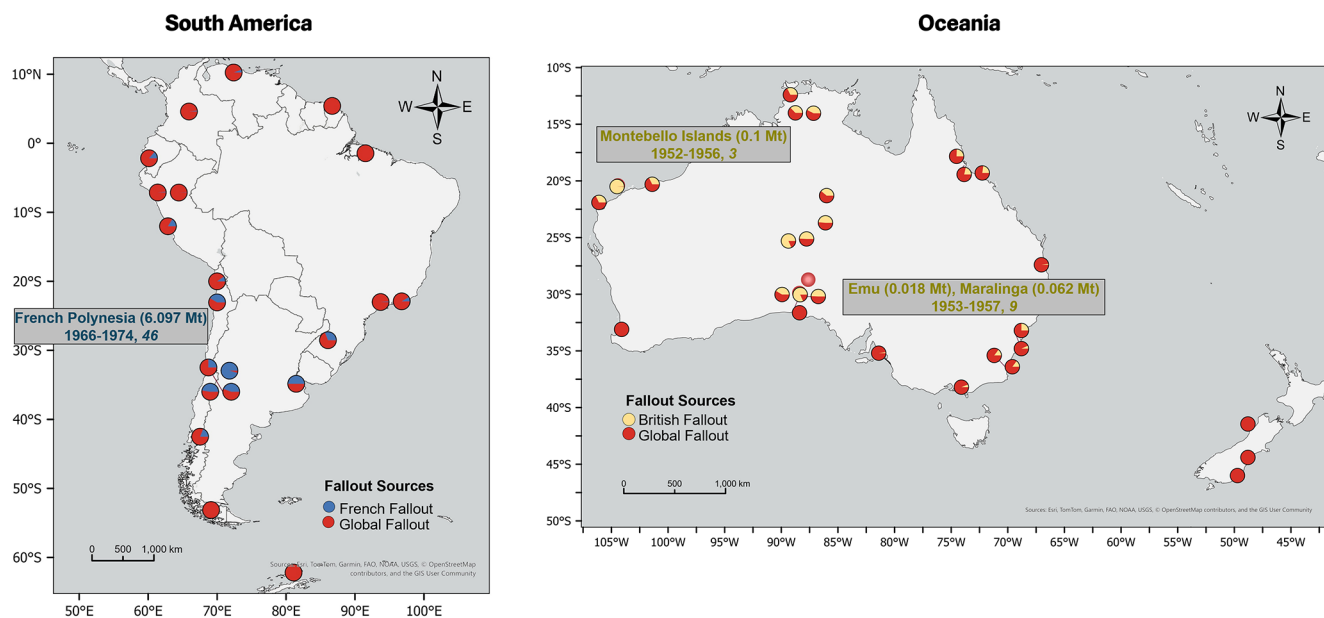


Figure 8. Relative contribution of the fallout sources in South America and Oceania, where there is a considerable contribution of the French and British fallout sources. See Fig. 4 for the exact location of testing sites. The information shown was sourced from Esri, TomTom, NOAA, USGS, © OpenStreetMap contributors, and the GIS User Community.

The heterogeneity associated with the contribution from different NWT sources for $^{239+240}\text{Pu}$ inventories is certainly less significant than the heterogeneity associated with NPP accidents for ^{137}Cs (Alewell et al., 2017). However, it is still critical to address the uncertainties mentioned previously, especially in areas with a significant input of sources other than the global fallout when employing $^{239+240}\text{Pu}$ invento-

ries and isotopic ratios for a specific application. This has recently been demonstrated by Dowell et al. (2024a, b), who used $^{239+240}\text{Pu}$ inventories to assess soil erosion in western Kenya, wherein the low variability in the $^{239+240}\text{Pu}$ inventories and isotopic ratios were considered to be criteria for the suitability of the assessment technique. As such, the AVATAR-Soils Database provides a data compilation that

might be used to assess the heterogeneities of different regions.

6 Predicting ^{137}Cs and $^{239+240}\text{Pu}$ inventories in equatorial and Southern Hemisphere reference soils

The results of the random forest model for ^{137}Cs and $^{239+240}\text{Pu}$ are presented in Fig. 9. For ^{137}Cs , the most important covariate was precipitation during the coldest quarter, followed by longitude, annual precipitation, elevation, and latitude (Fig. 9b). In the case of $^{239+240}\text{Pu}$, mean diurnal temperature range emerged as the most important covariate, followed by precipitation during the driest quarter, annual temperature range, precipitation during the driest month, and precipitation seasonality (Fig. 9d). Due to the differences in the spatial coverage of ^{137}Cs and $^{239+240}\text{Pu}$ inventory data, with $^{239+240}\text{Pu}$ covering only sparse areas, different covariates emerged with different levels of importance. However, this does not imply that ^{137}Cs and $^{239+240}\text{Pu}$ are transported differently. As the $^{137}\text{Cs}/^{239+240}\text{Pu}$ activity ratios suggest (Table 1), ^{137}Cs and $^{239+240}\text{Pu}$ appear to follow similar deposition patterns for every fallout source.

In addition to precipitation, spatial variables like latitude and longitude emerged as important covariates. Latitude governs the deposition of FRNs from the troposphere through latitudinally constrained atmospheric circulation cells (UN-SEAR, 2000), while longitude is related to the location of test sites in the Southern Hemisphere. Elevation and temperature-related variables also emerged as important factors, as these govern the orographic processes that influence the deposition of FRNs (Meusburger et al., 2020).

Generally, precipitation is reported to account for about 90 % of FRN deposition (Wright et al., 1999) through the scavenging of particulates released from NWT (Mercer et al., 1963; Machta, 1964). However, Earth's atmospheric circulation is not uniform, with wind patterns converging and diverging at different locations globally, leading to an uneven distribution of FRNs in the atmosphere. As such, the relationship between precipitation and FRN inventories is only consistent within climatologically uniform areas (Chappell et al., 2011). This is apparent from the varying correlations observed between precipitation and ^{137}Cs inventories in different regions like the Arctic (Wright et al., 1999; Pálsson et al., 2006), South America (Chaboche et al., 2021; Chamizo et al., 2011), and Australia (Chappell et al., 2011). This also implies that other variables influence the global variability in ^{137}Cs and $^{239+240}\text{Pu}$ inventories.

The optimal mtry values were determined to be 8 for ^{137}Cs and 6 for $^{239+240}\text{Pu}$. Cross-validation of the random forest model yielded concordance correlation coefficients (CCC) of 0.74 for ^{137}Cs and 0.78 for $^{239+240}\text{Pu}$, with coefficients of determination (R^2) of 0.62 and 0.67, respectively. The root-mean-square error (RMSE) values were 200.2 for ^{137}Cs and

13.08 for $^{239+240}\text{Pu}$ (Fig. 9a and c). These findings demonstrate the potential of these data for developing future baseline maps of ^{137}Cs and $^{239+240}\text{Pu}$.

7 Data limitations, uncertainties, and recommendations

Compiling the data for the AVATAR-Soils Database was connected to inherent data limitations that could not be avoided due to uncertainties and obscurities in the reviewed publications. The criteria used for reference soils are often not explicitly reported, which made it challenging to verify. Thus, we report the criteria that we used to define a reference soil, the vegetation at the time of sampling, and land-use history, if available. As much as possible, the coordinates of the soil profiles were taken as provided by the authors; however, the accuracy varied across different publications. While more recent publications provided highly accurate coordinates, the coordinates provided in older publications might be connected to lower accuracy due to limitations in technology. For example, the coordinates provided in Hardy et al. (1972, 1973) were expressed only up to the 10th decimal place, resulting in some points falling outside of land surface areas when mapped in ArcGIS Pro. These points were, therefore, not used in the random forest implementation. Some older publications (e.g., Loughran et al., 1989, 1992, 1993) have also only provided maps that lack longitudinal and latitudinal axes. In these cases, the maps were overlaid in Google Earth to extract the coordinates. A further limitation was that some published data were only presented as figures. These figures were, therefore, digitized via WebPlotDigitizer v4.5 (Rohatgi, 2020), which provides only an approximation of the exact values used by the authors.

As ^{137}Cs and $^{239+240}\text{Pu}$ were measured in different laboratories using different analytical techniques (for $^{239+240}\text{Pu}$), which are connected to different measurement uncertainties, another source of uncertainty is introduced when comparing the data compiled. In addition, the heterogeneity of samples used for analysis, as pointed out by previous studies (Kelley et al., 1999; Chamizo et al., 2020), may also affect the representativeness of the values reported. Finally, ^{137}Cs data without the sampling date or date of decay correction were decay-corrected using the average time delay between sampling and publication. Users of the AVATAR-Soils Database must, therefore, be aware of the abovementioned limitations. We also recommend that all important information related to ^{137}Cs and $^{239+240}\text{Pu}$ be made available in future publications to increase the accuracy of the data. This includes a sufficient description of the sampling area, date of measurement or decay correction (for ^{137}Cs), analytical precision, uncertainties, and detection limits.

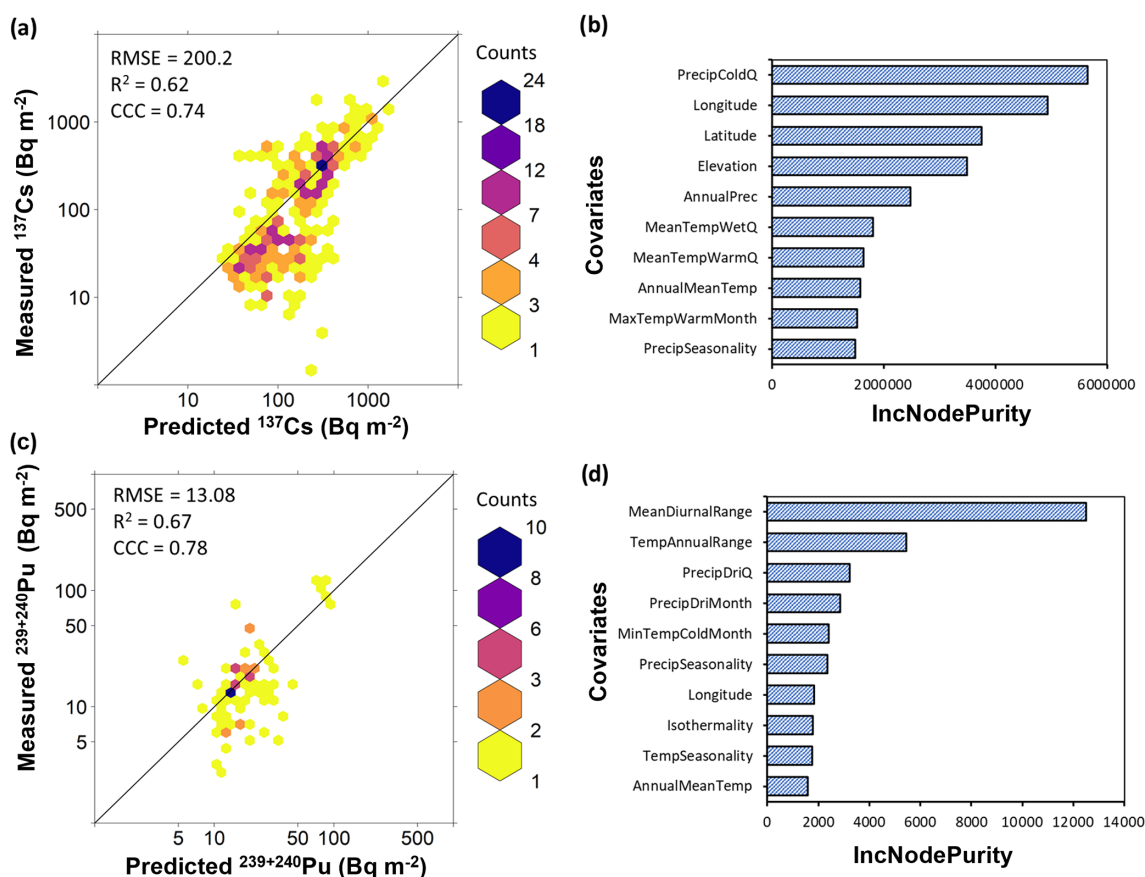


Figure 9. Results derived from the random forest model. Panels (a) and (c) show the correlation between measured and cross-validation predictions of ^{137}Cs and $^{239+240}\text{Pu}$, respectively. The color gradient represents the number of observations within each hexagonal bin, with the solid black line indicating the 1 : 1 relationship. Panels (b) and (d) present the relative importance of covariates in modeling ^{137}Cs and $^{239+240}\text{Pu}$. The x axis shows the average increase in node purity, with higher values indicating greater importance. The top 10 most significant covariates (full names listed in Table S1) are displayed in the plot.

8 Data availability

The AVATAR-Soils Database may be accessed from the Zenodo repository: <https://doi.org/10.5281/zenodo.14008221> (Dicen et al., 2024).

9 Code availability

Codes used for running the statistics and modeling were written in R and are available upon request from the corresponding author.

10 Conclusions and outlook

Current scientific knowledge on ^{137}Cs and $^{239+240}\text{Pu}$ is better constrained in the Northern Hemisphere, and there are many uncertainties, especially regarding their distribution, their sources, and the factors that govern their distribution, in the Southern Hemisphere. The AVATAR-Soils Database is – to the best of our knowledge – the first comprehensive

compilation of ^{137}Cs and $^{239+240}\text{Pu}$ data in equatorial and Southern Hemisphere reference soils from the literature.

The meta-analysis results revealed that high ^{137}Cs and $^{239+240}\text{Pu}$ inventories were recorded near the Equator and within the 20–40° S latitudinal bands, which coincide with the latitudes at which many NWT events were conducted. The $^{240}\text{Pu}/^{239}\text{Pu}$ atomic ratios suggest that sources other than the global fallout (primarily from US and USSR weapons testing with a $^{240}\text{Pu}/^{239}\text{Pu}$ atomic ratio of ~ 0.18) contributed to the reference inventories in the Southern Hemisphere, especially in South America and Oceania. The French fallout had a significant contribution between 20 and 40° S in South America, which is around the same latitude at which the French NWT events were conducted in Polynesia. In Australia, a significant contribution of the British fallout can be observed in the central and western parts of the country, in zones near and between the testing sites in Emu, Maralinga, and the Montebello Islands. However, lake sediment data should be investigated to confirm whether or not the areas affected by the French and British fallout, which has sim-

ilar $^{240}\text{Pu}/^{239}\text{Pu}$ atom ratios but different fallout chronologies, are indeed geographically well delineated.

Via a modeling approach, we identified the most important set of climatic, topographic, and spatial variables that can predict the ^{137}Cs and $^{239+240}\text{Pu}$ inventories. The common predictors for both ^{137}Cs and $^{239+240}\text{Pu}$ were precipitation during the driest quarter, longitude, mean diurnal range, and other temperature-related variables. Despite the good predictability of inventories using these variables, actual inventories must still be measured in areas that lack data to further strengthen and improve the model. Through this, we will be able to develop a more comprehensive understanding of the distribution and sources of ^{137}Cs and $^{239+240}\text{Pu}$ in equatorial and Southern Hemisphere soils and improve their application as tools in Earth science research.

Supplement. The supplement related to this article is available online at <https://doi.org/10.5194/essd-17-1529-2025-supplement>.

Author contributions. GD and CA conceptualized and designed the research. GD wrote the initial draft of the paper and revised the subsequent versions. SG developed the machine learning part of the study. CA provided overall supervision. All authors contributed to reviewing and editing the manuscript.

Competing interests. The contact author has declared that none of the authors has any competing interests.

Disclaimer. Publisher's note: Copernicus Publications remains neutral with regard to jurisdictional claims made in the text, published maps, institutional affiliations, or any other geographical representation in this paper. While Copernicus Publications makes every effort to include appropriate place names, the final responsibility lies with the authors.

Acknowledgements. The authors are grateful to the researchers who generously shared the actual data used in their publications, including Adrian Chappell (Cardiff University), Stephen Tims (The Australian National University), Rajeev Lal (The Australian National University), and Gerald Raab (University of Graz). We also thank the University of Basel students Lara Brunner, Magdalena Samland, Salome Wehrli, and Linda Agnetti, who dedicated time and effort to help us extract data from the selected articles.

Financial support. The AVATAR project is funded by the Swiss National Science Foundation (SNSF; grant no. 212886) and the French National Research Agency (ANR; grant no. ANR-22-CE93-0001).

Review statement. This paper was edited by Giulio G. R. Iovine and reviewed by two anonymous referees.

References

- Alewell, C., Meusburger, K., Juretzko, G., Mabit, L., and Ketterer, M. E.: Suitability of $^{239+240}\text{Pu}$ and ^{137}Cs as tracers for soil erosion assessment in mountain grasslands, *Chemosphere*, 103, 274–280, <https://doi.org/10.1016/j.chemosphere.2013.12.016>, 2014.
- Alewell, C., Pitois, A., Meusburger, K., Ketterer, M., and Mabit, L.: $^{239+240}\text{Pu}$ from “contaminant” to soil erosion tracer: Where do we stand?, *Earth-Sci. Rev.*, 172, 107–123, <https://doi.org/10.1016/j.earscirev.2017.07.009>, 2017.
- Aoyama, M., Hirose, K., and Igarashi, Y.: Re-construction and updating our understanding on the global weapons tests ^{137}Cs fallout, *J. Environ. Monit.*, 8, 431–438, <https://doi.org/10.1039/B512601K>, 2006.
- Arata, L., Meusburger, K., Bürge, A., Zehring, M., Ketterer, M. E., Mabit, L., and Alewell, C.: Decision support for the selection of reference sites using ^{137}Cs as a soil erosion tracer, *Soil*, 3, 113–122, <https://doi.org/10.5194/soil-3-113-2017>, 2017.
- Bennett, B. G.: Worldwide dispersion and deposition of radionuclides produced in atmospheric tests, *Health Phys.*, 82, 644–655, <https://doi.org/10.1097/00004032-200205000-00011>, 2002.
- Bertine, K. K., Chow, T. J., Koide, M., and Goldberg, E. D.: Plutonium isotopes in the environment: Some existing problems and some new ocean results, *J. Environ. Radioactiv.*, 3, 189–201, [https://doi.org/10.1016/0265-931X\(86\)90025-1](https://doi.org/10.1016/0265-931X(86)90025-1), 1986.
- Bouisset, P., Nohl, M., Bouville, A., and Leclerc, G.: Inventory and vertical distribution of ^{137}Cs , $^{239+240}\text{Pu}$, and ^{238}Pu in soil from Raivavae and Hiva Oa, two French Polynesian islands in the southern hemisphere, *J. Environ. Radioactiv.*, 183, 82–93, <https://doi.org/10.1016/j.jenvrad.2017.12.017>, 2018.
- Bouisset, P., Nohl, M., Cossonnet, C., Boulet, B., Thomas, S., Cariou, N., and Salaun, G.: Contribution of close-in fallout from the French atmospheric tests in inventories of ^{137}Cs , ^{241}Am , and plutonium (238 , 239 , 240) in Gambier Islands (French Polynesia)-Signatures of stratospheric fallout in the Southern Hemisphere, *J. Environ. Radioactiv.*, 235, 106624, <https://doi.org/10.1016/j.jenvrad.2021.106624>, 2021.
- Bouville, A.: Fallout from nuclear weapons tests: environmental, health, political, and sociological considerations, *Health Phys.*, 118, 360–381, <https://doi.org/10.1097/hp.0000000000001237>, 2020.
- Breiman, L.: Random forests, *Mach. Learn.*, 45, 5–32, <https://doi.org/10.1023/A:1010933404324>, 2001.
- Brode, H. L.: A review of nuclear explosion phenomena pertinent to the effects of nuclear weapons, RAND Corporation, <https://www.rand.org/content/dam/rand/pubs/reports/2007/R425.pdf> (last access: 9 April 2025), 1964.
- Bruel, R. and Sabatier, P.: serac: An R package for Shortlived RADionuclide chronology of recent sediment cores, *J. Environ. Radioactiv.*, 225, 106449, <https://doi.org/10.1016/j.jenvrad.2020.106449>, 2020.
- Buesseler, K. O.: The isotopic signature of fallout plutonium in the north Pacific, *J. Environ. Radioactiv.*, 36, 69–83, [https://doi.org/10.1016/S0265-931X\(96\)00071-9](https://doi.org/10.1016/S0265-931X(96)00071-9), 1997.

- Campbell, B. L., Loughran, R. J., and Elliott, G. L.: Caesium-137 as an indicator of geomorphic processes in a drainage basin system, *Aust. Geogr.*, 15, 49–64, <https://doi.org/10.1111/j.1467-8470.1982.tb00393.x>, 1982.
- Certini, G. and Scalenghe, R.: Soil is the best testifier of the diachronous dawn of the Anthropocene, *J. Plant Nutr. Soil Sc.*, 184, 183–186, <https://doi.org/10.1002/jpln.202000481>, 2021.
- Chaboche, P.-A., Saby, N. P. A., Laceby, J. P., Minella, J. P. G., Tiecher, T., Ramon, R. R., Tassano, M., Cabral, P., Cabrera, M., Bezerra da Silva, Y. J. A., Lefevre, I., and Evrard, O.: Mapping the spatial distribution of global ^{137}Cs fallout in soils of South America as a baseline for Earth Science studies, *Earth-Sci. Rev.*, 214, 103542, <https://doi.org/10.1016/j.earscirev.2021.103542>, 2021.
- Chamizo, E., García-León, M., Peruchena, J. I., Cereceda, F., Vidal, V., Pinilla, E., and Miró, C.: Presence of plutonium isotopes, ^{239}Pu and ^{240}Pu , in soils from Chile, *Nucl. Instrum. Meth. B*, 269, 3163–3166, <https://doi.org/10.1016/j.nimb.2011.04.021>, 2011.
- Chamizo, E., Rääf, C., López-Lora, M., García-Tenorio, R., Holm, E., Rabesiranana, N., and Pédehontaa-Hiaa, G.: Insights into the Pu isotopic composition ^{239}Pu , ^{240}Pu , and ^{241}Pu and ^{236}U in marshland samples from Madagascar, *Sci. Total Environ.*, 740, 139993, <https://doi.org/10.1016/j.scitotenv.2020.139993>, 2020.
- Chappell, A., Hancock, G., Viscarra Rossel, R. A., and Loughran, R.: Spatial uncertainty of the ^{137}Cs reference inventory for Australian soil, *J. Geophys. Res.-Earth*, 116, F04014, <https://doi.org/10.1029/2010JF001942>, 2011.
- Chiappini, R., Taillade, J.-M., and Brébion, S.: Development of a high-sensitivity inductively coupled plasma mass spectrometer for actinide measurement in the femtogram range, *J. Anal. Atom. Spectrom.*, 11, 497–503, <https://doi.org/10.1039/JA9961100497>, 1996.
- Chiappini, R., Millies-Lacroix, J. C., Le Petit, G., and Pointurier, F.: $^{240}\text{Pu}/^{239}\text{Pu}$ isotopic ratios and $^{239+240}\text{Pu}$ total measurements in surface and deep waters around Mururoa and Fangataufa Atolls compared with Rangiroa Atoll (French Polynesia), in: *Proceedings of the International Symposium on Marine Pollution*, Vienna, Austria, 7–11 September 1998, 147–149, <https://inis.iaea.org/records/av572-09p38> (last access: 9 April 2025), 1998.
- Chiappini, R., Pointurier, F., Millies-Lacroix, J. C., Lepetit, G., and Hemet, P.: $^{240}\text{Pu}/^{239}\text{Pu}$ isotopic ratios and $^{239+240}\text{Pu}$ total measurements in surface and deep waters around Mururoa and Fangataufa atolls compared with Rangiroa atoll (French Polynesia), *Sci. Total Environ.*, 237, 269–276, [https://doi.org/10.1016/S0048-9697\(99\)00141-2](https://doi.org/10.1016/S0048-9697(99)00141-2), 1999.
- Child, D. P. and Hotchkis, M. A. C.: Plutonium and uranium contamination in soils from former nuclear weapon test sites in Australia, *Nucl. Instrum. Meth. B*, 294, 642–646, <https://doi.org/10.1016/j.nimb.2012.05.018>, 2013.
- Corcho-Alvarado, J., Steinmann, P., Estier, S., Bochud, F., Haldimann, M., and Froidevaux, P.: Anthropogenic radionuclides in atmospheric air over Switzerland during the last few decades, *Nat. Commun.*, 5, 3030, <https://doi.org/10.1038/ncomms4030>, 2014.
- Cornell, R. M.: Adsorption of cesium on minerals: a review, *J. Radioanal. Nucl. Ch.*, 171, 483–500, <https://doi.org/10.1007/BF02219872>, 1993.
- de Bortoli, M., Gaglione, P., Malvicini, A., and Van Der Stricht, E.: Plutonium-239 and 238, strontium-90 and cesium-137 in surface air from mid 1961 through 1965, in: *Proc. First Int. Congr. Radiat. Prot.*, 361–367, Elsevier, <https://doi.org/10.1016/B978-1-4832-8312-8.50067-9>, 1968.
- de Lima Ferreira, P. A., Figueira, R. C. L., Siegle, E., Neto, N. E. A., de Castro Martins, C., Schettini, C. A. F., and de Mahiques, M. M.: Using a cesium-137 (^{137}Cs) sedimentary fallout record in the South Atlantic Ocean as a supporting tool for defining the Anthropocene, *Anthropocene*, 14, 34–45, <https://doi.org/10.1016/j.ancene.2016.06.002>, 2016.
- Dicen, G., Guillevic, F., Gupta, S., Chaboche, P.-A., Meusburger, K., Sabatier, P., Evrard, O., and Alewell, C.: AVATAR-Soils Database: A Database of ^{137}Cs and $^{239+240}\text{Pu}$ in Equatorial and Southern Hemisphere Reference Soils (1.0), Zenodo [data set], <https://doi.org/10.5281/zenodo.14008221>, 2024.
- Dowell, S. M., Humphrey, O. S., Gowing, C. J., Barlow, T. S., Chenery, S. R., Isaboke, J., Blake, W. H., Osano, O., and Watts, M. J.: Suitability of ^{210}Pb , ^{137}Cs and $^{239+240}\text{Pu}$ as soil erosion tracers in western Kenya, *J. Environ. Radioact.*, 271, 107327, <https://doi.org/10.1016/j.jenvrad.2023.107327>, 2024a.
- Dowell, S., Humphrey, O., Isaboke, J., Barlow, T., Blake, W., Osano, O., and Watts, M.: Plutonium isotopes can be used to model soil erosion in Kenya, *Environ. Geochem. Hlth.*, 46, 338, <https://doi.org/10.1007/s10653-024-02084-2>, 2024b.
- Everett, S. E., Tims, S. G., Hancock, G. J., Bartley, R., and Fifield, L. K.: Comparison of Pu and ^{137}Cs as tracers of soil and sediment transport in a terrestrial environment, *J. Environ. Radioact.*, 99, 383–393, <https://doi.org/10.1016/j.jenvrad.2007.10.019>, 2008.
- Evrard, O., Chaboche, P. A., Ramon, R., Foucher, A., and Laceby, J. P.: A global review of sediment source fingerprinting research incorporating fallout radiocesium (^{137}Cs), *Geomorphology*, 362, 107103, <https://doi.org/10.1016/j.geomorph.2020.107103>, 2020.
- Evrard, O., Bryskere, O., Skonieczny, C., Foucher, A., Bizeul, R., Chalaux Clergue, T., Barbier, J.-S., Petit, J.-E., Corcho-Alvarado, J. A., Röllin, S., Chaboche, P.-A., and Orizaola, G.: Was the ^{137}Cs contained in Saharan dust deposited across Europe in March 2022 emitted by French nuclear tests in Algeria?, *EGU General Assembly 2023*, Vienna, Austria, 24–28 Apr 2023, EGU23-1303, <https://doi.org/10.5194/egusphere-egu23-1303>, 2023.
- Ferraro, J. V., Hoggarth, J. A., Zori, D., Binetti, K. M., and Stinchcomb, G.: Integrating human activities, archeology, and the paleo-critical zone paradigm, *Front. Earth Sci.*, 6, 84, <https://doi.org/10.3389/feart.2018.00084>, 2018.
- Fick, S. E. and Hijmans, R. J.: WorldClim 2: new 1 km spatial resolution climate surfaces for global land areas, *Int. J. Climatol.*, 37, 4302–4315, <https://doi.org/10.1002/joc.5086>, 2017.
- Foucher, A., Chaboche, P.-A., Sabatier, P., and Evrard, O.: A worldwide meta-analysis (1977–2020) of sediment core dating using fallout radionuclides including ^{137}Cs and ^{210}Pb s, *Earth Syst. Sci. Data*, 13, 4951–4966, <https://doi.org/10.5194/essd-13-4951-2021>, 2021.
- Foucher, A., Tassano, M., Chaboche, P.-A., Chalar, G., Cabrera, M., Gonzalez, J., Cabral, P., Simon, A.-C., Agelou, M., Ramon, R., Tiecher, T., and Evrard, O.: Inexorable land degradation due to agriculture expansion in South American Pampa, *Nat. Sustain.*, 6, 662–670, <https://doi.org/10.1038/s41893-023-01074-z>, 2023.

- Froehlich, M. B., Akber, A., McNeil, S. D., Tims, S. G., Fifield, L. K., and Wallner, A.: Anthropogenic ^{236}U and Pu at remote sites of the South Pacific, *J. Environ. Radioact.*, 205, 17–23, <https://doi.org/10.1016/j.jenvrad.2019.05.003>, 2019.
- Garcia Agudo, E.: Global distribution of ^{137}Cs inputs for soil erosion and sedimentation studies, in: Use of ^{137}Cs in the Study of Soil Erosion and Sedimentation, Proceedings of the Consultants Meeting on the Use of ^{137}Cs in the Study of Soil Erosion and Sedimentation, Vienna, Austria, 13–16 November 1995, IAEA-TECDOC-1028, 117–121, <https://www.osti.gov/etdweb/servlets/purl/640529> (last access: 7 April 2025), 1998.
- Guillevic, F., Gastineau, R., Evrard, O., Sabatier, P., Chaboche, P. A., Foucher, A., Bardelle, A., Achaga, R., Ruiz-Fernandez, A. C., Sanchez-Cabeza, J. A., Tassano, M., Cabrera, M., Chalar, G., Quincke, J. A., Moreno-Allende, V., Moernaut, J., Corcho Alvarado, J. A., Röllin, S., Sahli, H., Kobler, J., Dicen, G., and Alewell, C.: Using plutonium isotopes to identify French nuclear test fallout period (1966–1974): An additional time-marker for South America, Thirteenth International Conference on Methods and Applications of Radioanalytical Chemistry, Hawaii, 23–28 March 2025, Log 494, http://www.marconference.org/wp-content/uploads/MARXIII-Final-Version-Book_of_Abstracts-2-17-2025.pdf (last access: 8 April 2025), 2025.
- Gupta, S., Lehmann, P., Bonetti, S., Papritz, A., and Or, D.: Global prediction of soil saturated hydraulic conductivity using random forest in a covariate-based GeoTransfer function (CoGTF) framework, *J. Adv. Model. Earth Sy.*, 13, e2020MS002242, <https://doi.org/10.1029/2020MS002242>, 2021.
- Gupta, S., Papritz, A., Lehmann, P., Hengl, T., Bonetti, S., and Or, D.: Global mapping of soil water characteristics parameters – fusing curated data with machine learning and environmental covariates, *Remote Sens.*, 14, 1947, <https://doi.org/10.3390/rs14081947>, 2022.
- Hancock, G. J., Tims, S. G., Fifield, L. K., and Webster, I. T.: The release and persistence of radioactive anthropogenic nuclides, *Geol. Soc. Lond. Spec. Publ.*, 395, 265–281, <https://doi.org/10.1144/SP395.15>, 2014.
- Hardy Jr., E. P.: Fallout program. Quarterly summary report, September 1, 1974–December 1, 1974 (No. HASL-288), US-AEC Health and Safety Lab., New York, <https://www.osti.gov/biblio/4254369> (last access: 8 April 2025), 1975.
- Hardy, E.: Final tabulation of monthly Sr-90 fallout data, 1954–1976, USERDA Rep. HASL-329, <https://doi.org/10.2172/7291252>, 1977.
- Hardy, E. P., Krey, P. W., and Volchok, H. L.: Global inventory and distribution of fallout plutonium, *Nature*, 241, 444–445, <https://doi.org/10.1038/241444a0>, 1973.
- Hardy Jr., E. P., Krey, P. W., and Volchok, H. L.: Global inventory and distribution of ^{238}Pu from SNAP-9A, (No. HASL-250), New York Operations Office (AEC), NY Health and Safety Lab., <https://doi.org/10.2172/4689831>, 1972.
- Haukoos, J. S. and Lewis, R. J.: Advanced statistics: bootstrapping confidence intervals for statistics with “difficult” distributions, *Acad. Emerg. Med.*, 12, 360–365, <https://doi.org/10.1197/j.aem.2004.11.018>, 2005.
- Hodge, V., Smith, C., and Whiting, J.: Radiocesium and plutonium: Still together in “background” soils after more than thirty years, *Chemosphere*, 32, 2067–2075, [https://doi.org/10.1016/0045-6535\(96\)00108-7](https://doi.org/10.1016/0045-6535(96)00108-7), 1996.
- Hong, S. M., Yoon, I. H., and Cho, K. H.: Predicting the distribution coefficient of cesium in solid phase groups using machine learning, *Chemosphere*, 352, 141462, <https://doi.org/10.1016/j.chemosphere.2024.141462>, 2024.
- Hrnecek, E., Steier, P., and Wallner, A.: Determination of plutonium in environmental samples by AMS and alpha spectrometry, *Appl. Radiat. Isotopes*, 63, 633–638, <https://doi.org/10.1016/j.apradiso.2005.05.012>, 2005.
- Jagercikova, M., Cornu, S., Le Bas, C., and Evrard, O.: Vertical distributions of ^{137}Cs in soils: a meta-analysis, *J. Soils Sediments*, 15, 81–95, <https://doi.org/10.1007/s11368-014-0982-5>, 2015.
- Johansen, M. P., Child, D. P., Davis, E., Doering, C., Harrison, J. J., Hotchkis, M. A. C., Payne, T. E., Thiruvoth, S., Twining, J. R., and Wood, M. D.: Plutonium in wildlife and soils at the Maralinga legacy site: Persistence over decadal time scales, *J. Environ. Radioact.*, 131, 72–80, <https://doi.org/10.1016/j.jenvrad.2013.10.014>, 2014.
- Johansen, M. P., Child, D. P., Cresswell, T., Harrison, J. J., Hotchkis, M. A. C., Howell, N. R., Johansen, A., Sdraulig, S., Thiruvoth, S., Young, E., and Whiting, S. D.: Plutonium and other radionuclides persist across marine-to-terrestrial ecotopes in the Montebello Islands sixty years after nuclear tests, *Sci. Total Environ.*, 691, 572–583, <https://doi.org/10.1016/j.scitotenv.2019.06.531>, 2019.
- Jones, G. S.: Reactor-grade plutonium and nuclear weapons: ending the debate, *Nonprolif. Rev.*, 26, 61–81, <https://doi.org/10.1080/10736700.2019.1603497>, 2019.
- Kelley, J. M., Bond, L. A., and Beasley, T. M.: Global distribution of Pu isotopes and ^{237}Np , *Sci. Total Environ.*, 237, 483–500, [https://doi.org/10.1016/S0048-9697\(99\)00160-6](https://doi.org/10.1016/S0048-9697(99)00160-6), 1999.
- Kersting, A. B.: Plutonium transport in the environment, *Inorg. Chem.*, 52, 3533–3546, <https://doi.org/10.1021/ic3018908>, 2013.
- Ketterer, M. E. and Szechenyi, S. C.: Determination of plutonium and other transuranic elements by inductively coupled plasma mass spectrometry: a historical perspective and new frontiers in the environmental sciences, *Spectrochim. Acta B*, 63, 719–737, <https://doi.org/10.1016/j.sab.2008.04.018>, 2008.
- Kim, C. S., Lee, M. H., Kim, C. K., and Kim, K. H.: ^{90}Sr , ^{137}Cs , $^{239+240}\text{Pu}$, and ^{238}Pu concentrations in surface soils of Korea, *J. Environ. Radioact.*, 40, 75–88, [https://doi.org/10.1016/S0265-931X\(97\)00062-3](https://doi.org/10.1016/S0265-931X(97)00062-3), 1998.
- Kirchner, G.: Establishing reference inventories of ^{137}Cs for soil erosion studies: methodological aspects, *Geoderma*, 211, 107–115, <https://doi.org/10.1016/j.geoderma.2013.07.011>, 2013.
- Kirchner, G., Devell, L., Guntay, S., and K. H.: Radioactivity from Fukushima Dai-ichi in air over Europe; part 2: What can it tell us about the accident, *J. Environ. Radioact.*, 102, 35–40, <https://doi.org/10.1016/j.jenvrad.2011.12.016>, 2011.
- Koide, M., Michel, R., Goldberg, E. D., Herron, M. M., and Langway Jr., C. C.: Depositional history of artificial radionuclides in the Ross Ice Shelf, Antarctica, *Earth Planet. Sc. Lett.*, 44, 205–223, [https://doi.org/10.1016/0012-821X\(79\)90169-9](https://doi.org/10.1016/0012-821X(79)90169-9), 1979.
- Koide, M., Michel, R., Goldberg, E. D., Herron, M. M., and Langway, C. C.: Characterization of radioactive fallout from pre- and post-moratorium tests to polar ice caps, *Nature*, 296, 544–547, <https://doi.org/10.1038/296544a0>, 1982.

- Koide, M., Bertine, K. K., Chow, T. J., and Goldberg, E. D.: The $^{240}\text{Pu}/^{239}\text{Pu}$ ratio, a potential geochronometer, *Earth Planet. Sc. Lett.*, 72, 1–8, [https://doi.org/10.1016/0012-821X\(85\)90112-8](https://doi.org/10.1016/0012-821X(85)90112-8), 1985.
- Krey, P. W. and Beck, H. L.: Distribution throughout Utah of ^{137}Cs and $^{239+240}\text{Pu}$ from Nevada Test Site detonations, DOE/EML-400, U.S. Department of Energy, Environmental Measurements Laboratory, New York, <https://doi.org/10.2172/6854358>, 1981.
- Krey, P. W., Hardy, E. P., Pachucki, C., Rourke, F., Coluzza, J., and Benson, W. K.: Mass isotopic composition of global fall-out plutonium in soil, in: *Transuranium nuclides in the environment*, IAEA, Vienna, <https://inis.iaea.org/records/fg45k-3f759> (last access: 9 April 2025), 1976.
- Kurihara, Y., Takahata, N., Yokoyama, T. D., Miura, H., Kon, Y., Takagi, T., Higaki, S., Yamaguchi, N., Sano, Y., and Takahashi, Y.: Isotopic ratios of uranium and caesium in spherical radioactive caesium-bearing microparticles derived from the Fukushima Dai-ichi Nuclear Power Plant, *Sci. Rep.*, 10, 3281, <https://doi.org/10.1038/s41598-020-59933-0>, 2020.
- LaBrecque, J. and Cordoves, P.: Determination and spatial distribution of ^{137}Cs in soils, mosses and lichens near Kavanayen, Venezuela, *J. Radioanal. Nucl. Ch.*, 273, 401–404, <https://doi.org/10.1007/s10967-007-6847-2>, 2007.
- LaBrecque, J. J. and Rosales, P. A.: Erratum to “the preliminary results of the measurements of environmental levels of ^{40}K and ^{137}Cs in Venezuela” [*Nucl. Instr. Meth. A*, 312 (1992) 217], *Nucl. Instrum. Meth. A*, 332, 342–342, [https://doi.org/10.1016/0168-9002\(93\)90780-L](https://doi.org/10.1016/0168-9002(93)90780-L), 1993.
- Lachner, J., Christl, M., Bisinger, T., Michel, R., and Synal, H.-A.: Isotopic signature of plutonium at Bikini Atoll, *Appl. Radiat. Isotopes*, 68, 979–983, <https://doi.org/10.1016/j.apradiso.2010.01.043>, 2010.
- Lal, R., Fifield, L. K., Tims, S. G., and Wasson, R. J.: ^{239}Pu fallout across continental Australia: Implications on ^{239}Pu use as a soil tracer, *J. Environ. Radioactiv.*, 178, 394–403, <https://doi.org/10.1016/j.jenvrad.2017.08.009>, 2017.
- Lawrence, I. and Lin, K.: A concordance correlation coefficient to evaluate reproducibility, *Biometrics*, 45, 255–266, <https://doi.org/10.2307/2532051>, 1989.
- Lin, M., Qiao, J., Hou, X., Dellwig, O., Steier, P., Hain, K., Golser, R., and Zhu, L.: 70-year anthropogenic uranium imprints of nuclear activities in Baltic Sea sediments, *Environ. Sci. Technol.*, 55, 8918–8927, <https://doi.org/10.1021/acs.est.1c02136>, 2021.
- Loughran, R. J. and Balog, R. M.: Re-sampling for soil-caesium-137 to assess soil losses after a 19-year interval in a Hunter Valley vineyard, New South Wales, Australia, *Geogr. Res.*, 44, 77–86, <https://doi.org/10.1111/j.1745-5871.2006.00360.x>, 2006.
- Loughran, R. J., Campbell, B. L., and Elliott, G. L.: The identification and quantification of sediment sources using ^{137}Cs , in: *Proceedings of the Symposium on Recent Developments in the Explanation and Prediction of Erosion and Sediment Yield*, IAHS Publication No. 137, Exeter, UK, 19–23 July 1982, 361–369, 1982.
- Loughran, R. J., Elliott, G. L., Campbell, B. L., and Shelly, D. J.: Estimation of soil erosion from caesium-137 measurements in a small, cultivated catchment in Australia, *Int. J. Radiat. Appl. Instrum. A Appl. Radiat. Isotopes*, 39, 1153–1157, [https://doi.org/10.1016/0883-2889\(88\)90009-3](https://doi.org/10.1016/0883-2889(88)90009-3), 1988.
- Lujanienė, G., Valiulis, D., Byčėnienė, S., Šakalys, J., and Povinec, P. P.: Plutonium isotopes and ^{241}Am in the atmosphere of Lithuania: A comparison of different source terms, *Atmos. Environ.*, 61, 419–427, <https://doi.org/10.1016/j.atmosenv.2012.07.0468>, 2012.
- Mabit, L., Benmansour, M., and Walling, D. E.: Comparative advantages and limitations of the fallout radionuclides ^{137}Cs , ^{210}Pb , and ^7Be for assessing soil erosion and sedimentation, *J. Environ. Radioactiv.*, 99, 1799–1807, <https://doi.org/10.1016/j.jenvrad.2008.08.009>, 2008.
- Mabit, L., Meusburger, K., Fulajtar, E., and Alewell, C.: The usefulness of ^{137}Cs as a tracer for soil erosion assessment: A critical reply to Parsons and Foster (2011), *Earth-Sci. Rev.*, 127, 300–307, <https://doi.org/10.1016/j.earscirev.2013.05.008>, 2013.
- Mabit, L., Chhem-Kieth, S., Dornhofer, P., Toloza, A., Benmansour, M., Bernard, C., Fulajtar, E., and Walling, D. E.: ^{137}Cs : A widely used and validated medium term soil tracer, IAEA TECDOC SE-RIES, 27, <https://inis.iaea.org/records/2gg34-s9w48> (last access: 9 April 2025), 2014.
- Machta, L.: Meteorological processes in the transport of weapon radioiodine, in: *Biology of Radioiodine*, Elsevier, 43–52, <https://doi.org/10.1016/B978-1-4832-2890-7.50010-2>, 1964.
- McArthur, R. D. and Miller Jr, F. L.: Off-Site Radiation Exposure Review Project: Phase 2 Soils Program (No. DOE/NV/10384-23-Rev.), Nevada Univ., Las Vegas, NV (USA), Water Resources Center, <https://digital.library.unt.edu/ark:/67531/metadc1186734/> (last access: 9 April 2025), 1989.
- Meusburger, K., Mabit, L., Ketterer, M., Park, J. H., Sándor, T., Porto, P., and Alewell, C.: A multi-radionuclide approach to evaluate the suitability of $^{239+240}\text{Pu}$ as soil erosion tracer, *Sci. Total Environ.*, 566, 1489–1499, <https://doi.org/10.1016/j.scitotenv.2016.06.035>, 2016.
- Meusburger, K., Porto, P., Mabit, L., La Spada, C., Arata, L., and Alewell, C.: Excess Lead-210 and Plutonium-239+240: Two suitable radiogenic soil erosion tracers for mountain grassland sites, *Environ. Res.*, 160, 195–202, <https://doi.org/10.1016/j.envres.2017.09.020>, 2018.
- Meusburger, K., Evrard, O., Alewell, C., Borrelli, P., Cinelli, G., Ketterer, M., Mabit, L., Panagos, P., van Oost, K., and Ballabio, C.: Plutonium aided reconstruction of caesium atmospheric fallout in European topsoils, *Sci. Rep.*, 10, 11858, <https://doi.org/10.1038/s41598-020-68736-2>, 2020.
- Meusburger, K., Porto, P., Kobler Waldis, J., and Alewell, C.: Validating plutonium-239+240 as a novel soil redistribution tracer – a comparison to measured sediment yield, *SOIL*, 9, 399–409, <https://doi.org/10.5194/soil-9-399-2023>, 2023.
- Mooney, C. Z., Duval, R. D., and Duvall, R.: Bootstrapping: A non-parametric approach to statistical inference (No. 95), Sage, <https://uk.sagepub.com/en-gb/eur/book/bootstrapping> (last access: 9 April 2025), 1993.
- Mukai, H., Ohnuki, T., and Kozai, N.: Cesium adsorption/desorption behavior of clay minerals considering actual contamination conditions in Fukushima, *Sci. Rep.*, 6, 21543, <https://doi.org/10.1038/srep21543>, 2016.
- Owens, P. N., Blake, W. H., and Millward, G. E.: Extreme levels of fallout radionuclides and other contaminants in glacial sediment (cryoconite) and implications for downstream aquatic ecosystems, *Sci. Rep.*, 9, 12531, <https://doi.org/10.1038/s41598-019-48873-z>, 2019.

- R Core Team: R: A language and environment for statistical computing, R Foundation for Statistical Computing, Vienna, Austria, <https://www.R-project.org/> (last access: 7 April 2025), 2024.
- Rohatgi, A.: Webplotdigitizer (Version 4.5), GitHub [code], <https://github.com/automeris-io/WebPlotDigitizer> (last access: 9 April 2025), 2020.
- Romanenko, V. and Lujanienė, G.: Short review of plutonium applications for sediment transport studies, *J. Environ. Radioactiv.*, 257, 107066, <https://doi.org/10.1016/j.jenvrad.2022.107066>, 2023.
- Şahin, S.: Reply to “Remarks on the Plutonium-240 Induced Pre-Ignition Problem in a Nuclear Device”, *Nucl. Technol.*, 54, 431–432, <https://doi.org/10.13182/NT81-A32795>, 1981.
- Salminen-Paatero, S., Vira, J., and Paatero, J.: Measurements and modeling of airborne plutonium in Subarctic Finland between 1965 and 2011, *Atmos. Chem. Phys.*, 20, 5759–5769, <https://doi.org/10.5194/acp-20-5759-2020>, 2020.
- Saito-Kokubu, Y., Yasuda, K., Magara, M., Miyamoto, Y., Sakurai, S., Usuda, S., Yamazaki, H., and Yoshikawa, S.: Geographical distribution of plutonium derived from the atomic bomb in the eastern area of Nagasaki, *J. Radioanal. Nucl. Chem.*, 273, 183–186, <https://doi.org/10.1007/s10967-007-0733-9>, 2007.
- Schuller, P., Ellies, A., and Handl, J.: Influence of climatic conditions and soil properties on ^{137}Cs vertical distribution in selected Chilean soils, *J. Plant Nutr. Soil Sci.*, 160, 423–426, <https://doi.org/10.1002/jpln.19971600312>, 1997a.
- Schuller, P., Ellies, A., and Kirchner, G.: Vertical migration of fallout ^{137}Cs in agricultural soils from Southern Chile, *Sci. Total Environ.*, 193, 197–205, [https://doi.org/10.1016/S0048-9697\(96\)05338-7](https://doi.org/10.1016/S0048-9697(96)05338-7), 1997b.
- Shuryak, I.: Machine learning analysis of ^{137}Cs contamination of terrestrial plants after the Fukushima accident using the random forest algorithm, *J. Environ. Radioactiv.*, 241, 106772, <https://doi.org/10.1016/j.jenvrad.2021.106772>, 2022.
- Steffen, W., Broadgate, W., Deutsch, L., Gaffney, O., and Ludwig, C.: The trajectory of the Anthropocene: the great acceleration, *Anthropocene Rev.*, 2, 81–98, <https://doi.org/10.1177/2053019614564785>, 2015.
- Steinhauser, G., Brandl, A., and Johnson, T. E.: Comparison of the Chernobyl and Fukushima nuclear accidents: a review of the environmental impacts, *Sci. Total Environ.*, 470, 800–817, <https://doi.org/10.1016/j.scitotenv.2013.10.029>, 2014.
- Tims, S. G., Fifield, L. K., Hancock, G. J., Lal, R. R., and Hoo, W. T.: Plutonium isotope measurements from across continental Australia, *Nucl. Instrum. Meth. B*, 294, 636–641, <https://doi.org/10.1016/j.nimb.2012.07.010>, 2013a.
- Tims, S. G., Tsifakis, D., Srncik, M., Fifield, L. K., Hancock, G. J., and De Cesare, M.: Measurements of low-level anthropogenic radionuclides from soils around Maralinga, *EPJ Web Conf.*, 63, 03010, <https://doi.org/10.1051/epjconf/20136303010>, 2013b.
- UNSCEAR: Ionizing radiation: sources and biological effects, 1982 report to the General Assembly, with annexes, United Nations, New York, <https://doi.org/10.18356/34127272-en>, 1982.
- UNSCEAR: Sources and effects of ionizing radiation, UNSCEAR 2000 Report, Volume II, United Nations, New York, <https://doi.org/10.18356/47a75909-en>, 2000.
- Wallbrink, P. J., Murray, A. S., Olley, J. M., and Olive, L. J.: Determining sources and transit times of suspended sediment in the Murrumbidgee River, New South Wales, Australia, using fallout ^{137}Cs and ^{210}Pb , *Water Resour. Res.*, 34, 879–887, <https://doi.org/10.1029/97WR03471>, 1998.
- Walling, D. E.: Use of ^{137}Cs and other fallout radionuclide in soil erosion investigations: progress, problems and prospects, IAEA-TECDOC-1028, <https://inis.iaea.org/records/ws91b-wxq33> (last access: 9 April 2025), 1998.
- Walling, D. E., Zhang, Y., and He, Q.: Models for converting measurements of environmental radionuclide inventories (^{137}Cs , Excess ^{210}Pb , and ^7Be) to estimates of soil erosion and deposition rates (including software for model implementation), Department of Geography, University of Exeter, UK, <https://citeseerx.ist.psu.edu/document?repid=rep1&type=pdf&doi=7a614c29d75eb09e732e8d9ad5ca853ec3b38b66> (last access: 9 April 2025), 2007.
- Wang, X., Liu, F., Zhang, X., Tang, X., Xu, J., Huang, P., Wang, Y., and Jin, Z.: Asynchronized erosion effects due to climate and human activities on the central Chinese Loess Plateau during the Anthropocene and its implications for future soil and water management, *Earth Surf. Proc. Land.*, 47, 1238–1251, <https://doi.org/10.1002/esp.5313>, 2022.
- Warneke, T., Croudace, I. W., Warwick, P. E., and Taylor, R. N.: A new ground-level fallout record of uranium and plutonium isotopes for northern temperate latitudes, *Earth Planet. Sc. Lett.*, 203, 1047–1057, [https://doi.org/10.1016/S0012-821X\(02\)00930-5](https://doi.org/10.1016/S0012-821X(02)00930-5), 2002.
- Wright, M. N. and Ziegler, A.: ranger: A fast implementation of random forests for high dimensional data in C++ and R, *J. Stat. Softw.*, 77, 1–17, <https://doi.org/10.18637/jss.v077.i01>, 2017.
- Wright, S. M., Howard, B. J., Strand, P., Nylén, T., and Sickel, M. A. K.: Prediction of ^{137}Cs deposition from atmospheric nuclear weapons tests within the Arctic, *Environ. Pollut.*, 104, 131–143, [https://doi.org/10.1016/S0269-7491\(98\)00140-7](https://doi.org/10.1016/S0269-7491(98)00140-7), 1999.